NUMERICAL MODELING OF SEAWATER-FRESH GROUNDWATER RELATIONSHIPS IN THE SELÇUK SUB-BASIN, İZMİR-TURKEY

A THESIS SUBMITTED TO

THE GRADUATE SCHOOL OF NATURAL AND APPLIED SCIENCES

OF

THE MIDDLE EAST TECHNICAL UNIVERSITY

BY

ABUBAKR HASSAN

IN PARTIAL FULFILLMENT OF THE REQUIREMENTS FOR THE DEGREE OF

MASTER OF SCIENCE

IN

THE DEPARTMENT OF GEOLOGICAL ENGINEERING

JANUARY 2004

Approval of the Graduate School of Natural and Applied Sciences

_____

Prof. Dr. Canan Özgen
Director

I certify that this thesis satisfies all the requirements as a thesis for the degree of Master of Science.

_____

Prof. Dr. Asuman Türkmenoğlu
Head of Department

This is to certify that we have read this thesis and that in our opinion it is fully adequate, in scope and quality, as a thesis for the degree of Master of Science.

_____

Assoc. Prof. Dr. Zeki Çamur

Supervisor

Examining Committee Members

Prof Dr. Vedat Doyuran (Chairman) _____

Prof. Dr. Hasan Yazıcıgil _____

Prof. Dr. Nurkan Karahanoğlu _____

Assoc. Prof. Dr. Zeki Çamur _____

Assoc. Prof. Dr. Mehmet Ekmekçi _____

ABSTRACT

NUMERICAL MODELING OF SEAWATER-FRESH GROUNDWATER RELATIONSHIPS IN THE SELÇUK SUB-BASIN, İZMİR-TURKEY

Hassan, Abubakr

M. Sc., Department of Geological Engineering
Superviser: Assoc. Prof. Dr. M. Zeki Çamur
January 2004, 67 pages

Seawater-fresh groundwater natural equilibrium conditions in the aquifers of the Selçuk sub-basin may be disturbed by the discharge occurred during the past 30 years in order to supply water for irrigation and domestic purpose usage. Two dimensional density dependent cross sectional saturated flow and solute transport simulations were carried out to determine whether seawater intrusion has occurred in the Selçuk sub-basin due to the imposed discharge or the determined salt-water in the western section of the aquifers represents natural interface equilibrium conditions. The numerical simulation model was calibrated using field measurements. The results of the simulations suggest that the seawater intrusion has occurred in the study area since the pumping activity increased in the region. Five scenarios were simulated for future predictions: (1) Present recharge and discharge conditions are maintained, (2) Discharge increases at a rate of the municipality need as a result of increasing population, (3) Discharge decreases by 12% from the present value, (4) Discharge decreases by 25% from the present value, and (5) No discharge occurs or recharge amount equals to the present discharge amount condition supplied to the aquifer. These scenario results suggest that seawater intrusion in the Selçuk sub-basin would progress in the following years unless proper management measures are taken into consideration.

KEYWORDS: seawater intrusion, density dependent groundwater flow, solute transport, contamination, Selçuk sub-basin.

ÖZ

SELÇUK ALT-HAVZASINDA DENİZ SUYU-YERALTISUYU İLİŞKİSİNİN SAYISAL MODELLEMESİ, İZMİR-TÜRKİYE

Hassan, Abubakr

Yüksek Lisans, Jeoloji Mühendisliği Bölümü
Tez Yöneticisi: Doç. Dr. M. Zeki Çamur
Ocak 2004, 67 sayfa

Selçuk alt-havzası akiferlerindeki deniz suyu-yeraltısuyu doğal denge koşullarının sulama ve günlük kullanım suyu temini amacıyla son 30 yıldır yapılan çekime bağlı olarak değişme olasılığı vardır. Selçuk alt-havzasında uygulanan yeraltusuyu çekiminin deniz suyu girişimine neden olup olmadığını veya akiferlerin batı bölgelerinde belirlenen tuzlu suyun doğal denge koşullarını yansıtıp yansıtmadığını belirlemek için, iki boyutlu yoğunluk bağımlı doygun akım ve iyon taşınım sayısal simülasyonları gerçekleştirildi. Sayısal simülasyon modeli saha ölçümleri ile kalibre edildi. Simülasyon sonuçları bölgede yeraltısuyu çekiminin artmasından bu yana çalışma sahasında deniz suyu girişimi olduğunu göstermektedir. Gelecek 20 yıl içerindeki durumu belirlemek amacıyla beş senaryo simülasyonu gerçekleştirilmiştir: (1) Günümüzdeki beslenim ve boşalım koşulları devam edecek, (2) Günümüzdeki çekim miktarı nüfus artışına bağlı olarak artacak, (3) Günümüzdeki çekim miktarı %12 azaltılacak, (4) Günümüzdeki çekim miktarı %25 azaltılacak ve (5) Günümüzdeki çekim tamamen durdurulacak veya söz konusu çekim miktarı kadar alt-havzaya beslenim sağlanacak. Bu senaryo sonuçları gerekli su yönetim planlaması yapılmadığı takdirde Selçuk alt-havzasındaki deniz suyu girişiminin devam edeceğini göstermektedir.

ANAHTAR KELİMELER: deniz suyu girişimi, yoğunluk bağımlı yeraltısuyu akımı, iyon taşınımı, kirlilik, Selçuk alt-havzası.

To My Parents
(Habibo and Hussein)

ACKNOWLEDGMENTS

I express my sincere appreciations to Assoc. Prof. Dr. Zeki Çamur, my supervisor, for his guidance, corrections, constructive criticism, and insight throughout the research.

Thanks go to the IDB (Islamic Development Bank) that provided me the financial support, which allowed my M.Sc. degree and this research come into the light.

Thanks also go to the Director of the State Hydraulic Works of Turkey, İzmir District Ahmed H. Alparslan for providing logistical support during field work of this thesis. I also express my appreciation to Prof. Dr. Asuman Türkmenoğlu for providing a study office during my thesis preparation. Thanks to Prof. Dr. Nurkan Karahanoğlu for his suggestions and comments.

The encouragements offered by Abdullah Cihan, Ismail Hassan and Mohamed Abyan are gratefully acknowledged.

TABLE OF CONTENTS

LIST OF TABLES

LIST OF FIGURES

CHAPTER 1

INTRODUCTION

1.1. Purpose and Scope

The Selçuk sub-basin located at the Aegean coast line at Selçuk, İzmir-Turkey was subjected to the seawater regression processes since 7th century BC (Erinç, 1978). The seawater regression was accompanied by protrusion, a freshwater cleaning up of the salt-water including aquifers, in the sub-basin since then.

Recent data of Yazıcıgil et al. (2000b), however, indicate that a salt-water problem is present in the western part of the Selçuk sub-basin aquifers. The natural equilibrium conditions may be disturbed by excessive discharge mainly for irrigation and domestic purpose use of groundwater in the region in the last 30 years. But it is not known that the presence of salt-water in the western parts of the aquifers is manifastation of the seawater-fresh groundwater natural equilibrium interface condition or indication of seawater intrusion processes due to excessive discharge.

The purpose of this study is to determine whether seawater intrusion occurring in the Selçuk sub-basin due to the imposed discharge and, if so, to assess the future trend of the seawater intrusion due to possible decrease/increase of recharge or increase of discharge caused by the increasing demand for groundwater.

The objectives of the study are as follows:

- Determination of present groundwater level and salt-water distributions in the aquifer through field measurements using available wells.
- Prediction of the pre-pumping (undisturbed) period groundwater level distribution in the Selçuk sub-basin using numerical simulations.
- Prediction of the pre-pumping period seawater-fresh groundwater interface position in the aquifer using numerical simulations.
- Prediction of the present groundwater level and chloride concentration distributions in the Selçuk sub-basin using numerical simulations.
- Assessment of future trend of the seawater intrusion in the area if the present condition continues without management interferences.
- Assessment of future trend of seawater intrusion in the area if the groundwater recharge is reduced/elevated or groundwater substraction increased/decreased.

These objectives (except the first one) will be achieved using saturated groundwater flow and solute mass transport numerical models.

1.2. Location and Extend of the Study Area

The Selçuk sub-basin is located within the Aegean Region at western Turkey between 4197000-4207000 North latitudes and 522000-536000 East longitudes (Figure 1.1). The sub-basin belongs to the Küçük Menderes River Basin (KMRB), situated within the provincial boundaries of the city of İzmir.

Study area

Figure 1.1 Location map of the Selçuk sub-basin.

1.3. Previous Studies

Several hydrogeological studies have been conducted in the KMRB. These works are briefly described below in a chronological order.

A geophysical resistivity survey, carried out to evaluate the groundwater resources in the KMRB, was reported by Gül (1967). The study covers the preparation of the depth to basement rock map, detection of the buried

faults, determination of the geometry of the units having aquifer characteristics, and determination of an areal extent of the Neogene sediments in the basin.

A study published by the State Hydraulic Works of Turkey (DSİ) in 1973 covers the first hydrogeological investigation in the KMRB. In this study, groundwater potential of the basin was investigated. The basin was divided into four regions as Selçuk plain, Kiraz plain, Tire-Ödemiş-Bayındır-Torbalı-Pancar plains, and Cumavası Plain. For each region, groundwater budget was estimated. In addition, a brief information concerning the geology, hydrogeology and groundwater quality of the aquifers was given.

The Japan International Cooperation agency (JICA) conducted a study between 1994 and 1996 (Nippon, 1996). The study deals with the preparation of a master plan for irrigation development in the KMRB. Moreover, the study was focused on the feasibility of the Beydağ Irrigation Project, putting main emphasis on the present conditions of socio-economy, agriculture, irrigation, agro-economy, and environment in and around the basin. In addition, the prospective land and water resources development plan, the environmental conservation program, a preliminary cost estimate of the Beydağ project and the proposed development and implementation program of the Beydağ Project were the subjects of the study. Groundwater modeling in the area was also first conducted by Nippon (1996). In this study, groundwater potential of the basin and the impact of the planned dams to the groundwater in the basin were specifically investigated.

Detailed hydrogeological, hydrochemical and geological investigations in the KMRB were carried out by Yazıcıgil et al. (2000a,b,c). Moreover, groundwater model and management scenarios were developed in this study. Existence of salt-water in the western section of the Selçuk sub-basin

aquifers was also shown in this work using depth wise groundwater quality measurements. The work aimed in this thesis, in fact, was stated by Yazıcıgil et al. (2000b) as one of the recommendations for future work to the State Hydraulic Works of Turkey.

CHAPTER 2

HYDROGEOLOGICAL CHARACTERISTICS OF THE STUDY AREA

2.1. Physiography

The Selçuk sub-basin is a plain bounded by the Aegean Sea from the west and by mountains from almost all other directions (Figure 2.1). The sub-basin is linked to the other sub-basins of the KMRB by a narrow passage through Belevi at Northeast. The Küçük Menderes River is the main drainage system in the Selçuk sub-basin area (Figure 2.2).

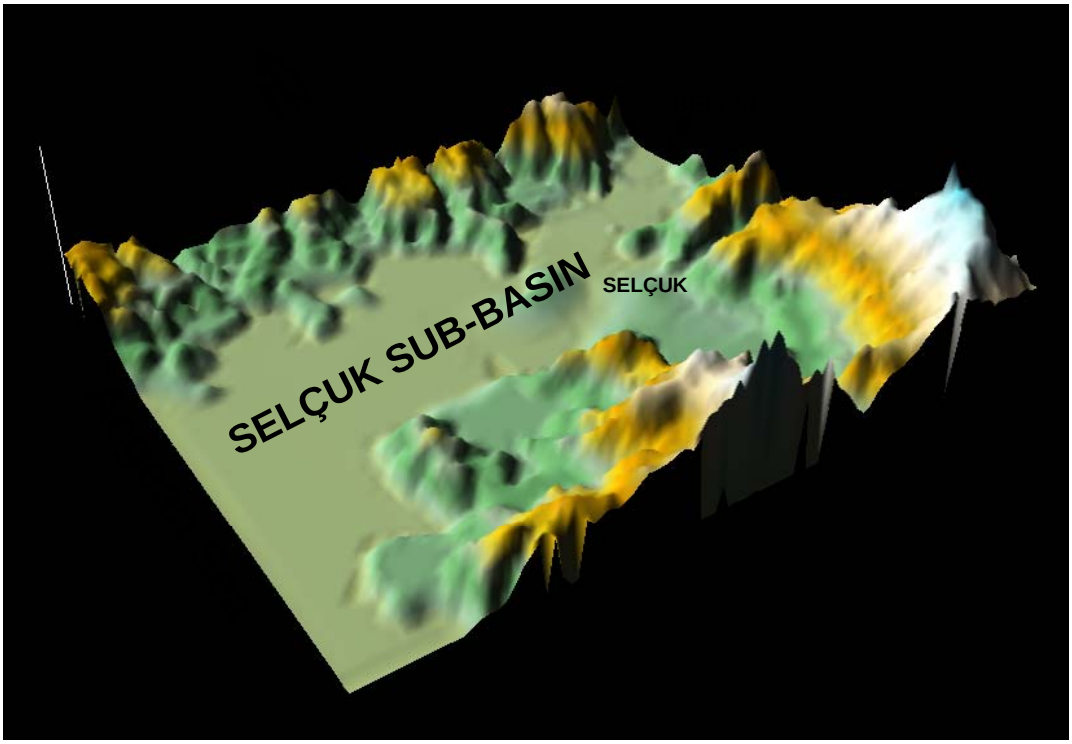

Figure 2.1 Elevation model of the Selçuk sub-basin.

2.2. Climate

The Selçuk sub-basin is located in the Aegean Sea climatic zone. In this zone, it is hot and dry in summer and mild and rainy in winter (Table 2.1). Data collected at the Selçuk meteorological station between the years of 1964 and 1997 indicate that annual means of temperature, precipitation, evaporation and humidity are about 16 ^{o}C, 688 mm, 1344 mm, and 63%, respectively. Monthly distributions of these annual mean values are listed in Table 2.1.

Table 2.1 Monthly mean temperature, precipitation, evaporation, and humidty values in the Selçuk sub-basin on the bases of 1964-1996 meteorological data.

	Jan.	Feb.	Mar.	Apr.	May	June	July	Aug.	Sep.	Oct.	Nov.	Dec.
Temperature (oC)	7.8	8.7	10.7	14.4	19.1	23.8	26.1	25.0	21.2	16.5	12.2	9.4
Precipitation (mm)	116.8	103.6	88.8	49.7	24.8	7.2	1.6	1.8	15.0	41.2	89.0	149.0
Evaporation (mm)	33.1	34.9	53.9	108.5	144.1	194.2	220.6	199.2	154.1	104.6	60.5	42.1
Humidity (%)	68	67	67	64	60	53	52	56	61	66	68	69

2.3. Geology

Geological characteristics of the Selçuk sub-basin summarized in this section are based on the work of Yazıcıgil et al. (2000c).

Metamorphic rocks, the oldest rock unit in the study area, belong to highly metamorphosed rock complex called the Menderes Massif. These basement rocks are overlain by either the Cretaceous Flysch, and/or the Neogene sedimentary rocks and/or the Quaternary alluvial deposits as shown in the geological map of the study area (Figure 2.2). The boundaries between metamorphic rocks and the Cretaceous Flysch and between the Cretaceous Flysch and the Neogene units are unconformable.

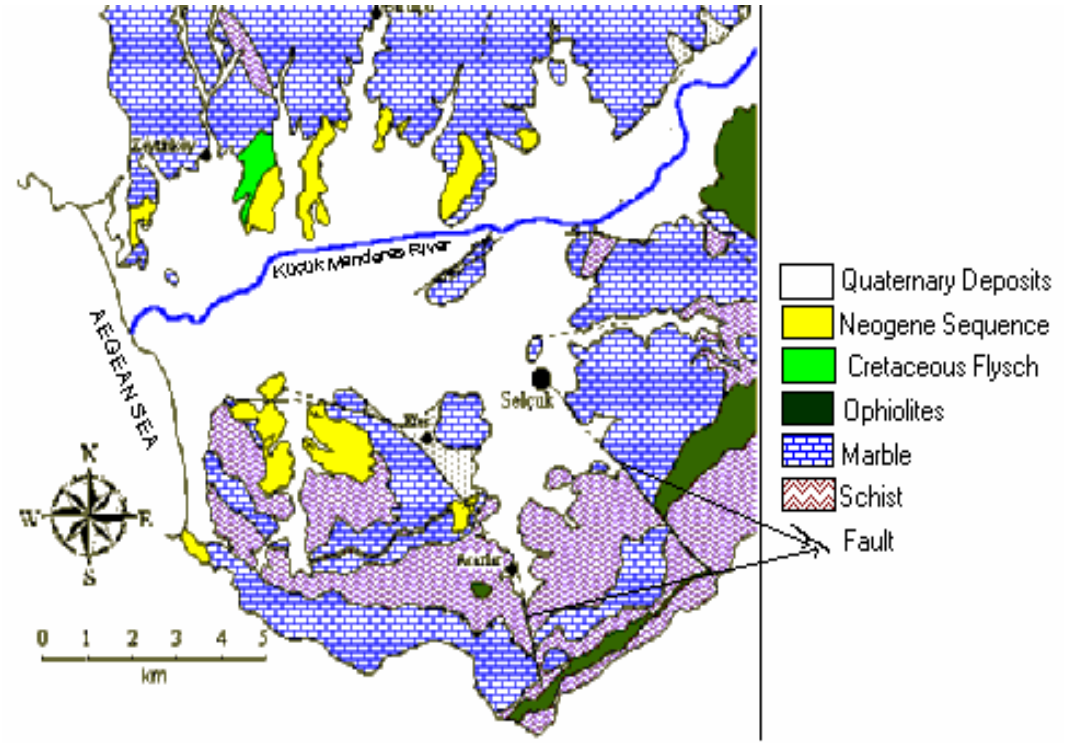

Figure 2.2 Geological map of the study area after Yazıcıgil et al. (2000c)

There are three main groups comprising the Menderes Massif complex: augen-gneisses, schist-phylites and marbles, stratigraphically the youngest unit of the metamorphic sequence. The Cretaceous Flysch is generally

characterized by a sequence of dark colored greywacke-conglomerate at lower parts, which grades into gray, massive dolomitic limestones toward top. The Neogene units are characterized by a sedimentary sequence grading from clastics to limestone and by acidic volcanics. The Quaternary sediments include alluvial fill and alluvial fans. The alluvial fill is the most widely distributed geologic unit in the Selçuk sub-basin and is composed of alternating of clay, silt, sand, and gravel. Black mud is also characteristic lithology at some locations indicating former swamp conditions. NW-SE oriented two faults extend from plain to highlands at southern section of the sub-basin (Figure 2.2).

2.4. Hydrogeology

Most of the hydrogeological characteristics of the units in the study area were obtained from well logs of the DSİ and İller Bankası (İB). Hydrogeological characteristics of the aquifers determined using these wells are listed in Table 2.2. Areal distribution of these wells in the sub-basin is shown in Figure 2.3.

Table 2.2a Well data for the Selçuk sub-basin. AF: Alluvial fan, AFI: Alluvial fill. Top: Topography.

Well no	Opening Date	East	North	Top(m)	Depth (m)	Filter (m)	Lithology
1000	Jul-60	532275	4200225	6	50		AFI
18495	Aug-73	533310	4201298	20.39	79	51-79	Marble
20045	Dec-75	533375	4201300	20	58.6	34.-58.6	Marble
20046	Feb-76	533325	4201450	20	105	33-105	Marble
20047	Feb-76	533225	4201450	20	86	56-86	Marble
21381	Oct-76	531093	4200396	6.47	74.6	44.-74.6	Marble

Table 2.2a (Continued).

Well no	Opening Date	East	North	Top (m)	Depth (m)	Filter (m)	Lithology
24853	Feb-79	531325	4200375	6	111	88.-111	Marble
24854	Mar-79	531500	4200380	6	156	32-100	AF+ AFI
24855	Apr-79	530875	4200300	6	60	14-60	Marble
54131	Jun-99	527750	4201925	2	161.5	56-156	AFI
54132	Jul-99	527750	4201825	2	268	162-268	Neogene
205	Jan-91	531375	4199075	15	52	28-48	AFI + Marble
221	Mar-91	531425	4199350	14	49	5-49	ABF+ Marbler
251	Mar-91	531700	4199600	10	72	28-64	ABF
254	Mar-91	531900	4199700	10.5	76	28-68	ABF
267	Mar-91	531300	4199625	10	35	13-35	Marble
639	Sep-85	526915	4198650	24	80	20-76	ABF+ Marble
652	Oct-95	526875	4198425	30	66	16-60	ABF+ Marble
984	Jun-88	533260	4201275	25	97	12-97	Marble
1021	Aug-88	533275	4201215	25	100	15.-100	Marble
1029	Aug-88	531400	4198775	20	70	19.-51.5	ABF
66(K1)	Sep-76	533225	4201225	25	90	9.5-90	Marble

Table 2.2b Well data for the Selçuk sub-basin.

WELL NO	DEPTH TO WATER(m)	STATIC LEVEL(m)	DYNAMIC LEVEL(m)	CAPACITY(l/s)	SPECIFIC CAPACI.(l/s/m)	TRANSMIS. (m^2/d)	PERMEABILITY (m^2) $X10^{-11}$	SPECIFIC YIELD
1000	8.55	-2.55	21.75	4	0.30			
18495	19.28	1.11	19.87	63	106.78	27688	131	0.4
20045	19.27	0.73	20.57	50	38.46	13167	68.7	
20046	18.34	1.66	19.15	57.5	70.99	90850	148.9	
20047	16.96	3.04	17.15	50	263.15	98750	388.4	
21381	5.4	1.07	6.32	52	56.52	27367	106.2	0.4
24853	4.83	1.17	5.22	60	153.85	94800	497.1	
24854	5.18	0.82	14.97	60	6.13	632	0.87	
24855	4.5	1.5	5.34	60	71.42	30800	79	
54131	1.98	0.02	2.7	10	13.9	347.2	0.38	
54132	3.9	-1.9	6.07	10	4.6	328	0.37	
205	16.4	-1.4	20	30	8.33	439.2	1.92	0.1
221	12.45	1.55	13.08	40	63.49	3504	11.5	0.15
251	10.12	-0.12	12.41	30	13.10	35	0.083	0.1
254	11	-0.5	25.33	7	0.49	174	0.48	0.1
267	12.9	-2.9	13.15	60	240	26480	143	
639	22.55	1.45	25.62	23	7.49	624	1.46	
652	7.8	22.2	25.13	8	0.46	32.4	0.11	
984	17.8	7.2						
1021	20.9	4.1	44.2	30	1.29	104	0.22	
1029	16.16	3.84	20.78	25	5.41	422.4	1.71	
66(K1)	17.62	7.38	20	62	26.05	3000	5.06	

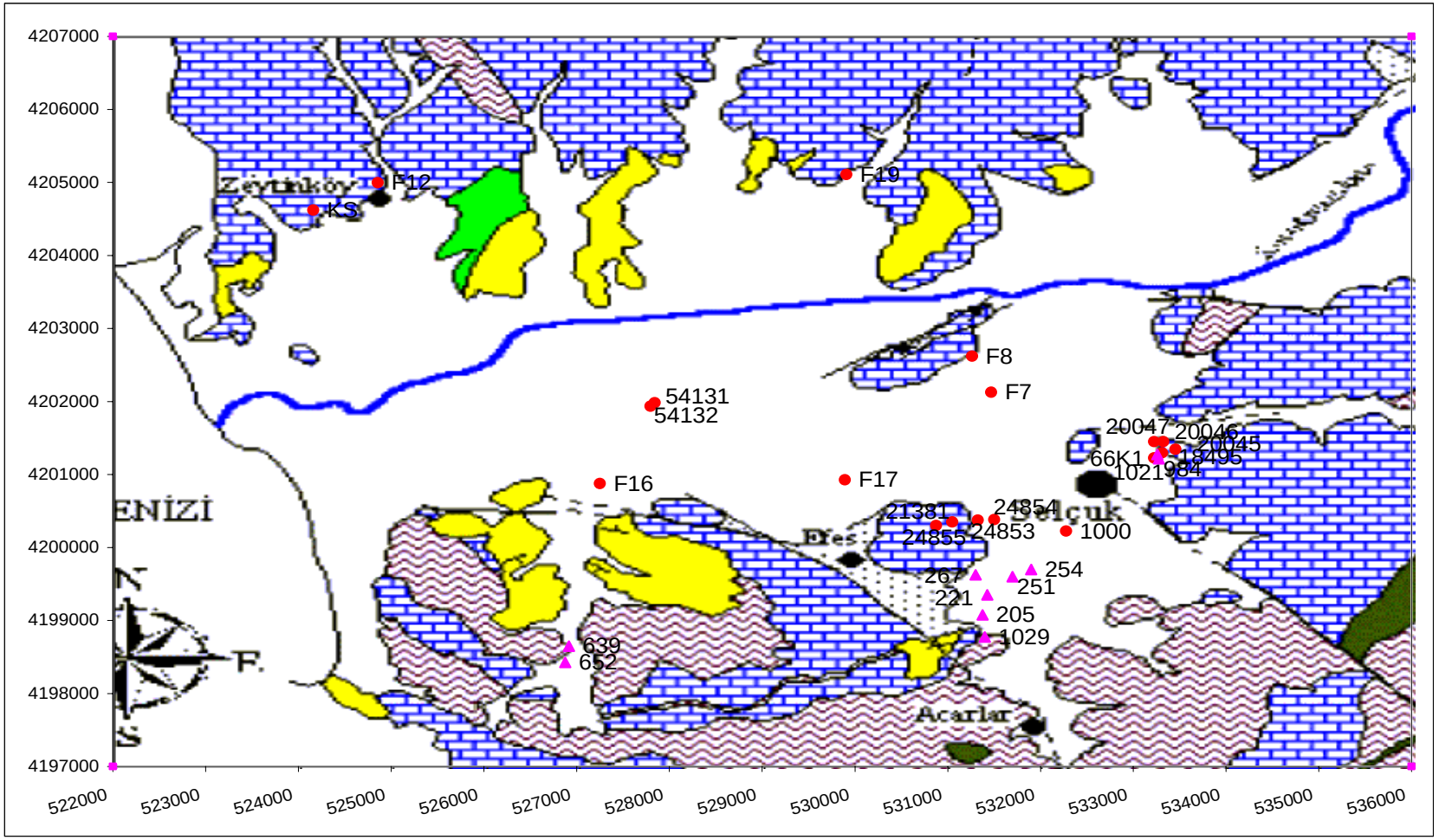

Figure 2.3 Distribution of wells and May, 2002 observation locations in the Selçuk sub-basin.

2.4.1. Hydrogeological Classification of Units

According to the previous studies (DSİ, 1973 and Yazıcıgil et al., 2000a,c), schists and ophiolites are impervious rocks and do not show aquifer characteristics. The marble unit, although it is part of the metamorphic complex, the secondary porosity and permeability produced by the presence of fractures and solution cavities in some locations, make it very productive aquifer. The average specific capacity of wells drilled in the marble unit is about 103 l/m/s. The permeability of the unit ranges from 0.22 x 10^{-11} m^2 to 497 x 10^{-11} m^2 with an average of 156 x 10^{-11} m^2 (Table 2.2). The marble unit has the highest average permeability among all the other units present in the Selçuk sub-basin. However the marble unit is not permeable in all locations.

There is only one well (no: 54132) filters the Neogene unit in the Selçuk sub-basin. The specific capacity and permeability of this well is 4.6 l/s/m and 0.37 x 10^{-11} m^2, respectively. The permeability of the Neogene units in the KMRB ranges from 0.24 x 10^{-11} m^2 to 2.4 x 10^{-11} m^2 (Yazıcıgil et al. 2000a).

The alluvial fill deposits constitute the main unconfined aquifer in the basin and cover the entire plain area. The deposits are generally composed of complex alternations of gravel, sand, silt, and clay materials. According to the wells located at the southern section of the sub-basin (excluding well no: 54131), the average specific capacity and permeability of the alluvial fill are about 5.1 l/s/m and 0.8 x 10^{-11} m^2 (Table 2.2). The permeability of the unit ranges from 0.08 x 10^{-11} m^2 to 1.7 x 10^{-11} m^2 at the southern section. There is only one well (no: 54131) located at the middle of the plain in the sub-basin. The permeability of the alluvial unit in this area is about 0.38 x 10^{-11} m^2 which is very similar to that of Neogene in the same location.

The storativity data in the area are scarce. The available data indicate specific yield of 0.1 for alluviual deposits and 0.4 for the marble units (Table 2.2).

2.4.2. Recharge

Average precipitation recharge to the aquifers in the Selçuk sub-basin was calculated by Gündoğdu (2000) based on the hydrological budget method using data collected between 1970 and 1995. In her work, 8 hm^3 net recharge was reported for 71.8 km^2 plain area and 6 hm^3 net recharge for 205.6 km^2 highland area of the sub-basin. Monthly distribution of average precipitation and recharge in the sub-basin are listed in Table 2.3.

Table 2.3 Monthly distribution of precipitation and recharge in the Selçuk sub-basin (Gündoğdu, 2000).

1964-1997		Jan.	Feb.	Mar	Apr	May	June
Average	(mm)	116.8	103.6	88.9	49.7	24.8	7.2
Precipitation	%	17	15	13	7.2	3.6	1
Average	ha	2.38	2.1	1.82	1.01	0.50	0.14
Recharge	Kg/s	75.48	66.60	57.72	31.97	15.98	4.44

1964-1997		July	Aug.	Sep.	Oct.	Nov.	Dec.	Total
Average	(mm)	1.6	1.8	15	41.2	89	149	688.4
Precipitation	%	0.2	0.2	2.2	6	13	21.6	100
Average	ha	0.03	0.03	0.31	0.84	1.82	3.02	14
Recharge	Kg/s	0.89	0.89	9.77	26.64	57.72	95.9	444

Additional recharge to the sub-basin aquifers takes place from the neighboring Bayındır-Torbalı sub-basin at northeast. Flow flux of 0.005567 m^3/day to the Selçuk sub-basin alluvial aquifer was calculated using 48410 m^2 cross sectional area by Yazıcıgil et al. (2000a).

Yazıcıgil et al. (2000a) reports for the KMRB that the Küçük Menderes River feeds the aquifers from November to June and the aquifers feeds the river from July to October. However, there is no available data about the Küçük Menderes river versus the aquifer flow relationships in the Selçuk sub-basin where the river flow conditions (e.g. flow velocity, discharge) are different from those of the other sub-basins. As it will be introduced in the following sections, equipotential lines are nearly perpendicular to the river flow direction in the Selçuk sub-basin, suggesting very low flow interaction between the river and the aquifer.

2.4.3. Discharge

Discharge of groundwater in the sub-basin has been accomplished through irrigation and domestic water supply since 1970 ies. Discharge for irrigation is estimated using the plant irrigation water need of Nippon (1996) and is listed in Table 2.4.

Table 2.4 Irrigation water need for a given month in the Selçuk sub-basin per km^2 area (Nippon, 1996).

Month	Plant Irrigation need (mm)	Kg/s
January	0.2	0.0063
February	0.5	0.0158

Table 2.4 (Continued)

Month	Plant Irrigation need (mm)	Kg/s
March	5.6	0.1775
April	22.1	0.7003
May	63.1	1.9995
June	108	3.4223
July	130.4	4.1321
August	137.7	4.3634
September	71.8	2.2752
October	18.1	0.5736
November	2.5	0.0792
December	0.4	0.0127
Total	560.4	17.7580

Wet (November-April) season and dry (May-October) season discharges per km^2 are calculated as 1 kg/s and 16.7 kg/s, respectively for irrigation. Since 1978, irrigation water at south is supplied to 240 ha area using cooperative I wells of 18495, 20045, 20046, and 20047. In the year of 1989, cooperative II wells 21381, 24853, 24854, and 24855 were also added to the discharge to irrigate 185 ha additional area at south. Irrigation water need at northern section of the sub-basin is pumped out using private wells.

Municipality water discharge is reported to be 2592000 m^3/y (82.2 kg/s) for the year of 1997 (Yazıcıgil et al, 2000a). 85 percent of this need is pumped out in dry season and the remaining is pumped out in wet season. Although there is no industrial discharge in the sub-basin, some establishments (e.g. gasoline stations, slaughter house, fire department) pump out groundwater

especially during dry season through their private wells whose discharge amounts are unknown.

2.4.4. Hydraulic Head Distribution in the Study Area

Low hydraulic head characterizes the study area because it is a coastal plain. The static levels measured at different dates in the DSİ wells are listed in Table 2.5. May 2002 data in the table were collected during fieldwork. The rest of the data in the table were compiled from DSİ (1973) and Yazıcıgil et al. (2000a). Based on May 2002 measurements, including private well data, groundwater table map of the area is approximated in Figure 2.4. In the area, groundwater levels of the two wells were also monthly monitored by the DSİ; well 18495 between 1973 and 1996 and well 21381 between 1976 and 1983. These data and hydrographs are given in Appendix A.

2.5. Hydrochemistry

Hydrochemical data compiled and collected by Yazıcıgil et al. (2000b) in the Selçuk sub-basin are listed in Appendix B. After spatial and temporal evaluation of the data, they concluded that salt-water is present at western section of the sub-basin but it is not possible to determine with the available data whether seawater intrusion has taken place.

Data collected in May 2002 during fieldwork include pH, electrical conductivity (EC), total dissolved solids (TDS), and salinity (S) measurements from 11 well locations (Table 2.6). The measurements were performed from pumped waters. Depths of wells are listed in Table 2.6. The spatial distribution of the EC at about 25 to 100 m depth of the aquifers in the sub-basin based on May 2002 data is approximated in Figure 2.5.

Table 2.5 Groundwater static levels in the Selçuk sub-basin.

WELL NO	EAST	NORTH	date (opening)	STATIC LEVEL (m)	date	STATIC LEVEL (m)	date	STATIC LEVEL (m)	date	STATIC LEVEL (m)	date	STATIC LEVEL (m)
20045	533375	4201300	Dec.75	0.73							May.02	0.205
20047	533225	4201450	Feb.76	3.04	Oct.98	-1.8	Apr.99	3.33	Oct.99	-0.65	May.02	1.665
21381	531093	4200396	Oct.76	1.07							May.02	1.505
24853	531325	4200375	Feb.79	1.17					Oct.99	-2.45	May.02	0.323
24854	531500	4200380	Mar.79	0.82	Oct.98	-3.345	Apr.99	0.86	Oct.99	-1.47	May.02	-0.13
24855	530875	4200300	Apr.79	1.5	Oct.98	-3.12	Apr.99	1.11	Oct.99	-2.15	May.02	0.301
54131	527750	4201925	Jun.99	0.02					Oct.99	0.31	May.02	1.245
54132	527750	4201825	Jul.99	-1.9					Oct.99	-0.38	May.02	0.67

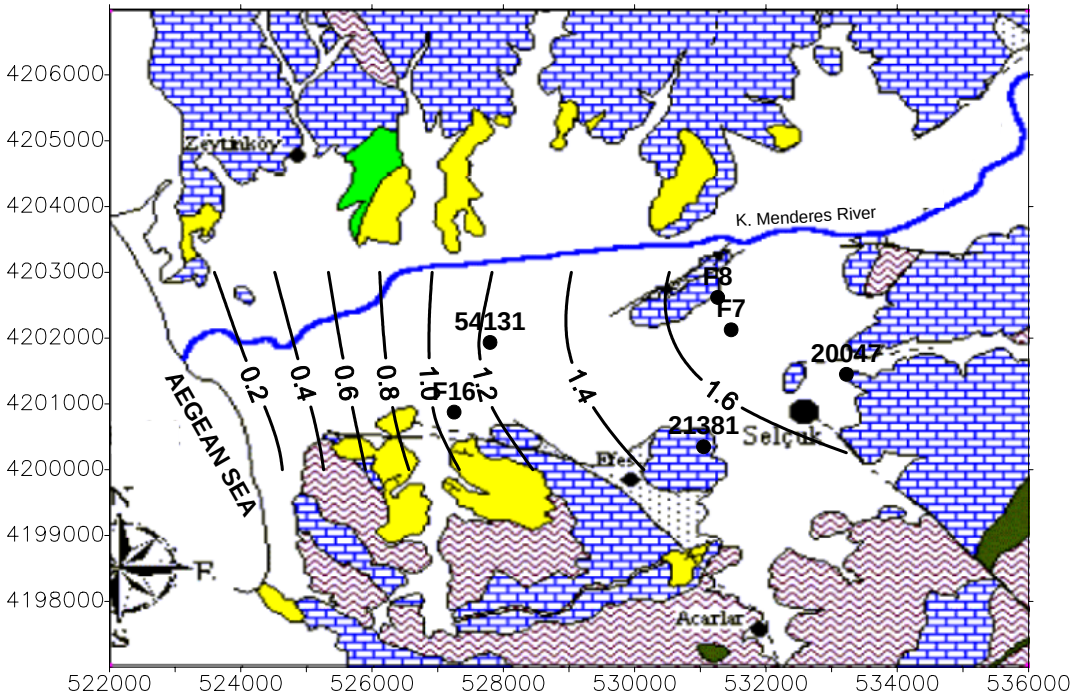

Figure 2.4 Groundwater table map of the Selçuk sub-basin in May 2002.

Table 2.6 Hydrochemical data collected in May 2002 fieldwork. KS: Kazancı spring. F: Private wells.

Well No	East	North	Depth (m)	pH	EC (µS/cm)	TDS (mg/l)	S (%)	T (^{o}C)
20045	533454	4201346	58.6	7.18	929	455		19.1
24854	531500	4200380	156	7.29	1418	703	0.7	19.2
21381	531050	4200350	74.6	7.04	2850	1454	1.5	20.6
24855	530875	4200300	60	7.06	2780	1417	1.4	20.7
F7	531470	4202127	120	7.51	3060	1567	1.6	19.8
F12	524856	4204997	30	7.05	1533	762	0.8	20.8
KS	524217	4204572	spring	7.05	5710	3010	3.1	19.3
F16	527250	4200876	-		9670	5260	5.4	18.7
F17	529892	4200926	-		1181	582	0.6	22.9
F19	529907	4205108	25	7.08	917	449	0.5	19.6
54131*	527797	4201935	160					
54132*	527841	4201981	268					

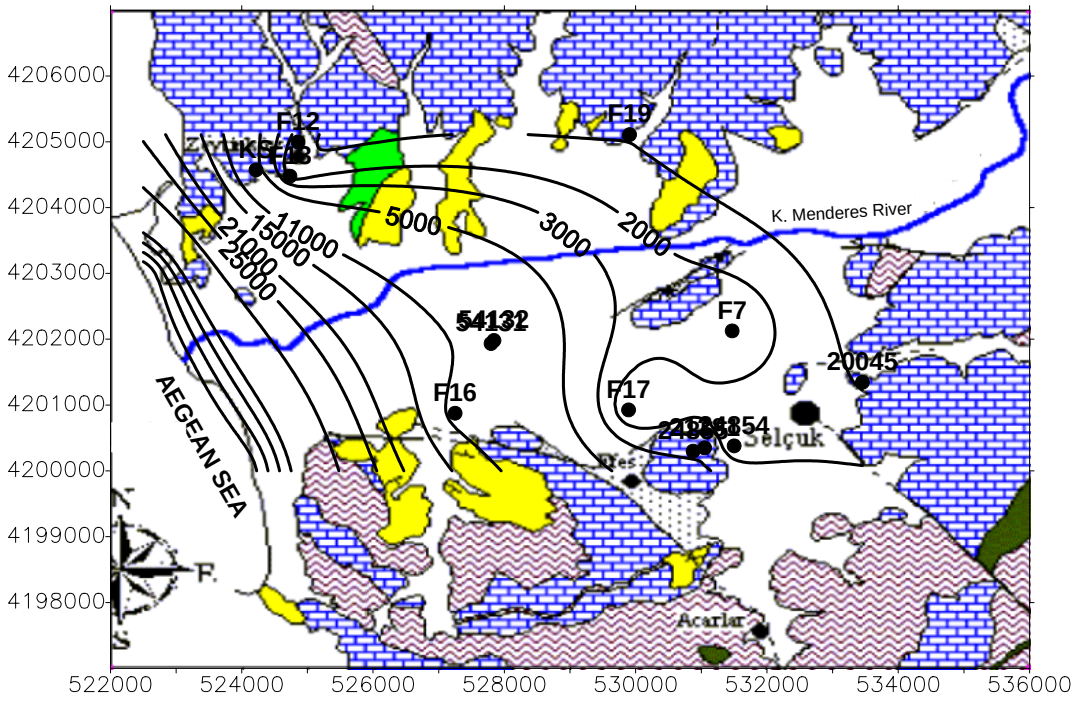

Figure 2.5 EC (µS/cm) distribution at a depth of 25-100 m in the Selçuk sub- basin in May 2002.

In addition to these pumped water measurements, depthwise EC profile measurements were also carried out from wells 54131 and 54132. The EC profiles determined in October 1999 by Yazıcıgil et al. (2000b) and in May 2002 field measurements are shown in Figure 2.6. Both profiles indicate the existence of saltwater interface in well 54131. As it can be seen from the figures, the EC values do not change considerably until the depth of about 100 m where the values increase sharply. The values level up again at a depth of about 125 m. Practically, there is no difference between the two profiles as expected because it is well established that the seawater intrusion and protrusion are slow processes.

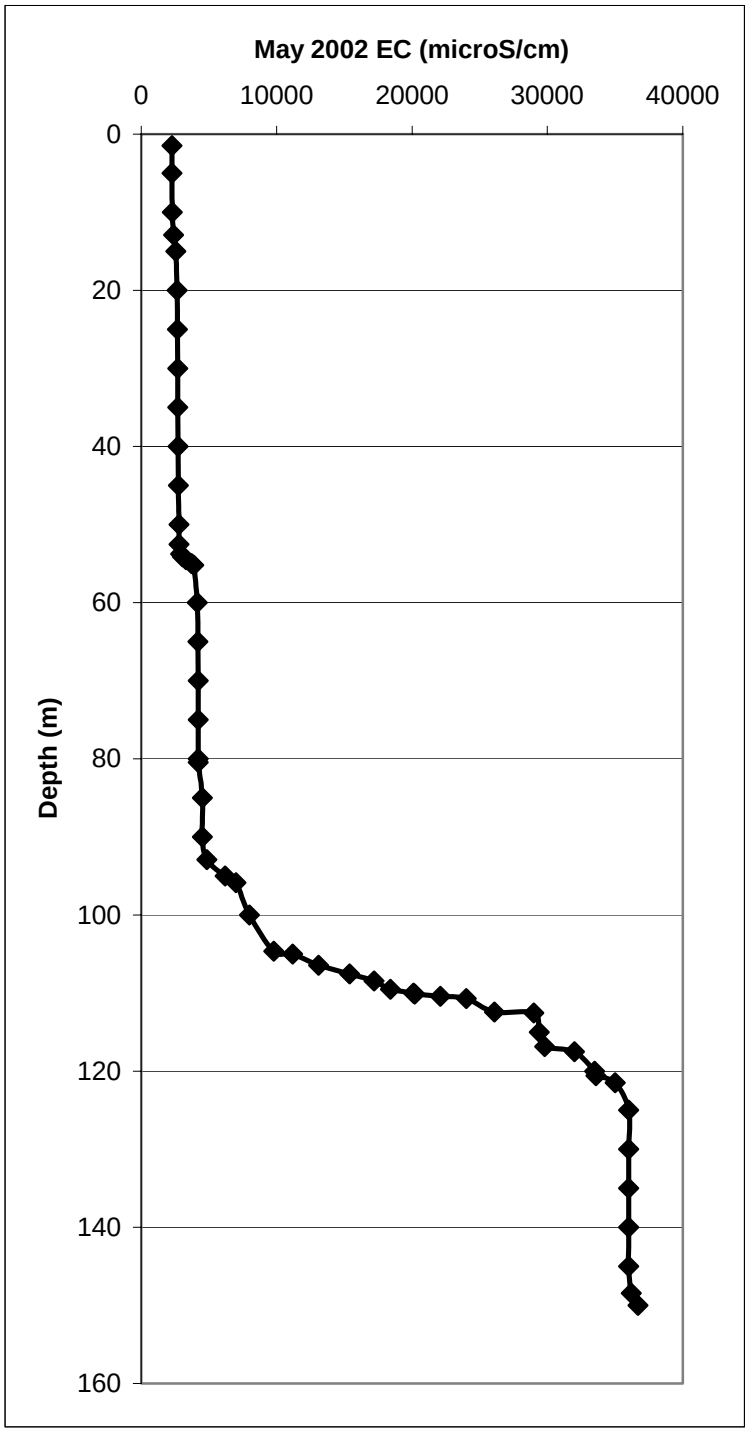

Figure 2.6a EC profile in well water of 54131 in May 2002.

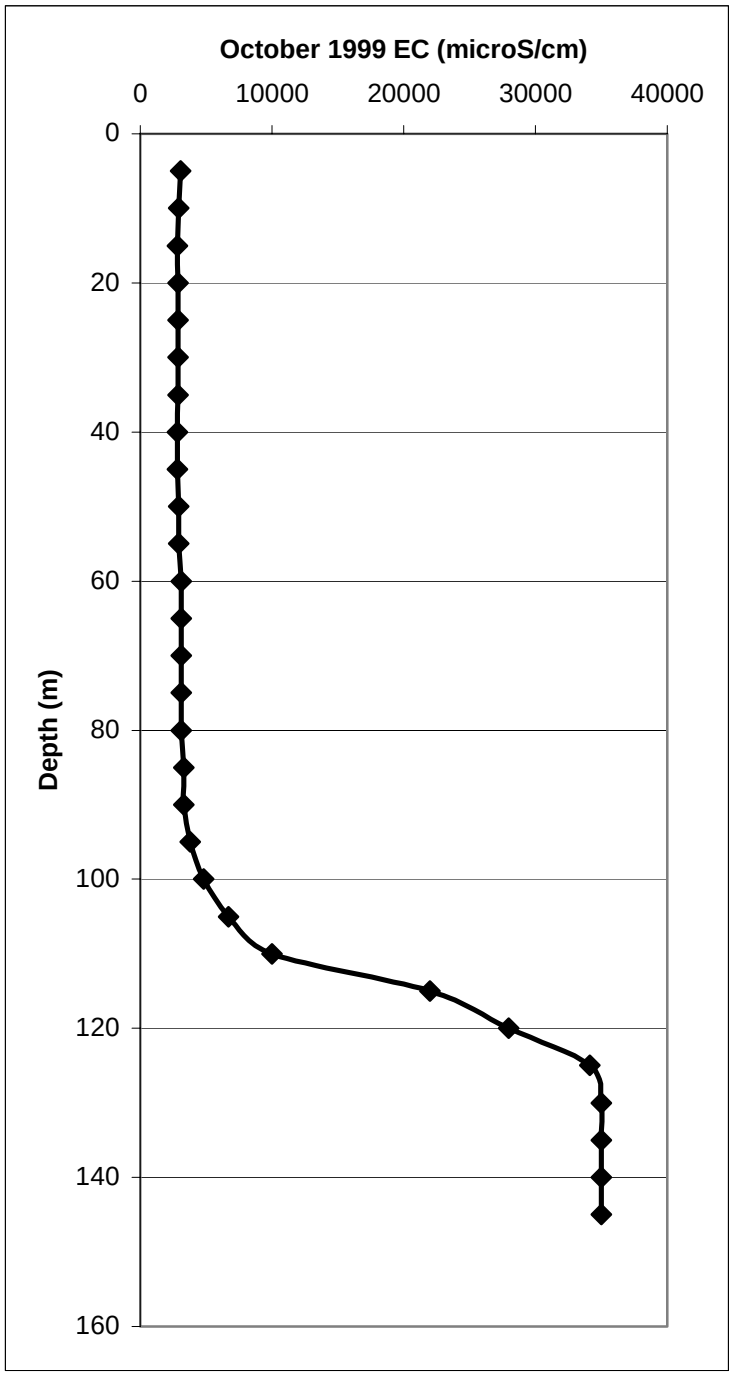

Figure 2.6b EC profile in well water of 54131 in October 1999 (Yazıcıgil et al., 2000b).

Well water of 54131 was also sampled at depths of 65 m, 110 m, and 140 m during May 2002 field work. Chloride concentrations measured in these samples and previous measurements are listed in Table 2.7.

In order to convert EC (μS/cm) profile data to Cl (mg/l) concentrations, best fit equations were obtained. The Cl profile estimated for May 2002 using the best fit equations are shown in Figure 2.7.

Table 2.7 Chloride concentration at various depths of well 54131.

54131			**54132**		
Date	**Depth (m)**	**Cl (mg/l)**	**Date**	**Depth (m)**	**Cl (mg/l)**
16.5.02	65	855	03.08.99	Pumped	15952
16.5.02	110	3660	03.08.99	Pumped	14640
16.5.02	140	14120	04.08.99	Pumped	15420

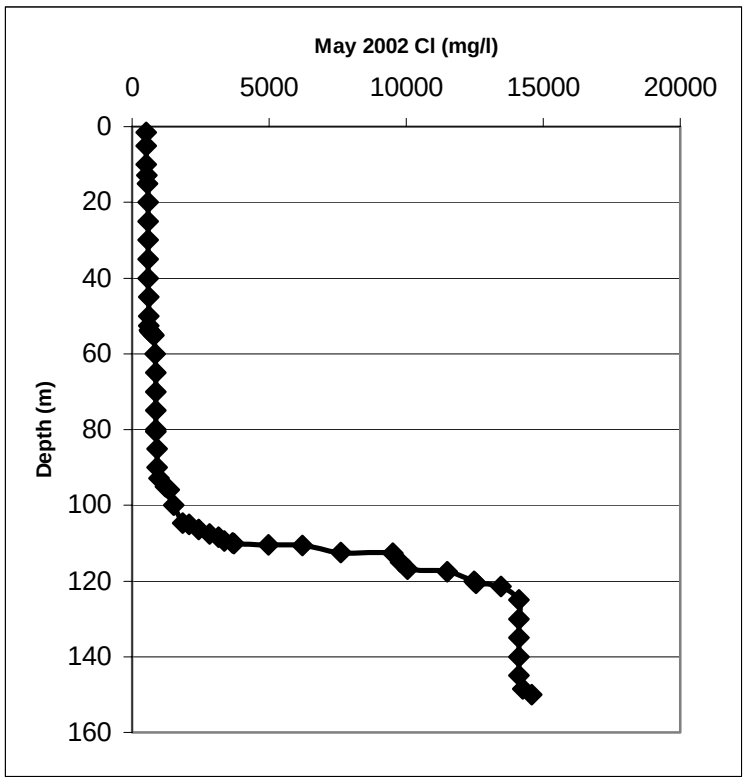

Figure 2.7. Estimated Cl concentration profile of 54131 well water in May 2002.

2.6. Surface Water

The major surface waters include the Küçük Menderes River and the Kazancı spring in the Selçuk sub-basin plain. Field work, carried out in May 2002 indicate that EC, TDS and S of the Küçük Menderes River are 756 mg/l, 1522 μS/cm, and 0.8 %0, respectively. The salinity of the river is less than the average groundwater salinity in the sub-basin (Table 2.6). The Kazancı spring situated at the northwest corner of the sub-basin nearby Zeytinköy village. During May, 2002 field work, it is measured that the EC of the spring is 5710 μS/cm, the TDS is 3010 mg/l and S is 3.1 %0, indicating high salinity in comparison to the salinity of groundwater pumped out from the wells in the sub-basin (Table 2.6).

CHAPTER 3

SALTWATER-FRESHWATER RELATIONSHIPS, THEORY AND HISTORICAL PERSPECTIVE

3.1. Theory of Saltwater-Freshwater Relationships

There are two models of simulation for saltwater-freshwater relationship, one of which is sharp interface approximation and the other approach is diffusive layer approximation.

The sharp interface method assumes that the saltwater and freshwater are immiscible fluids and mixing of the saltwater and freshwater by hydrodynamic dispersion is not considered. In other words, there is no transition zone or zone of mixing develops between the two fluids. In the mix or transition modeling approach, a zone of transition is allowed to develop between the salt-water and fresh water. The sharp interface is considered an appropriate approximation if the thickness of the transition zone is relatively small compared to the thickness of the aquifer (Bear, 1979). Reilly and Goodman (1987) suggested that a transition zone could be considered thin if it is less than one third of the thickness of the freshwater zone.

3.1.1. Ghyben-Herzberg Principle

The first quantitative approach to the saltwater depth in coastal porous aquifers was applied independently by Badon Ghyben (also written Ghijben)

in Netherland and by Herzberg in Northern Germany. They have introduced the simplest sharp interface model known as Badon Ghyben-Herzberg Principle (Figure 3.1).

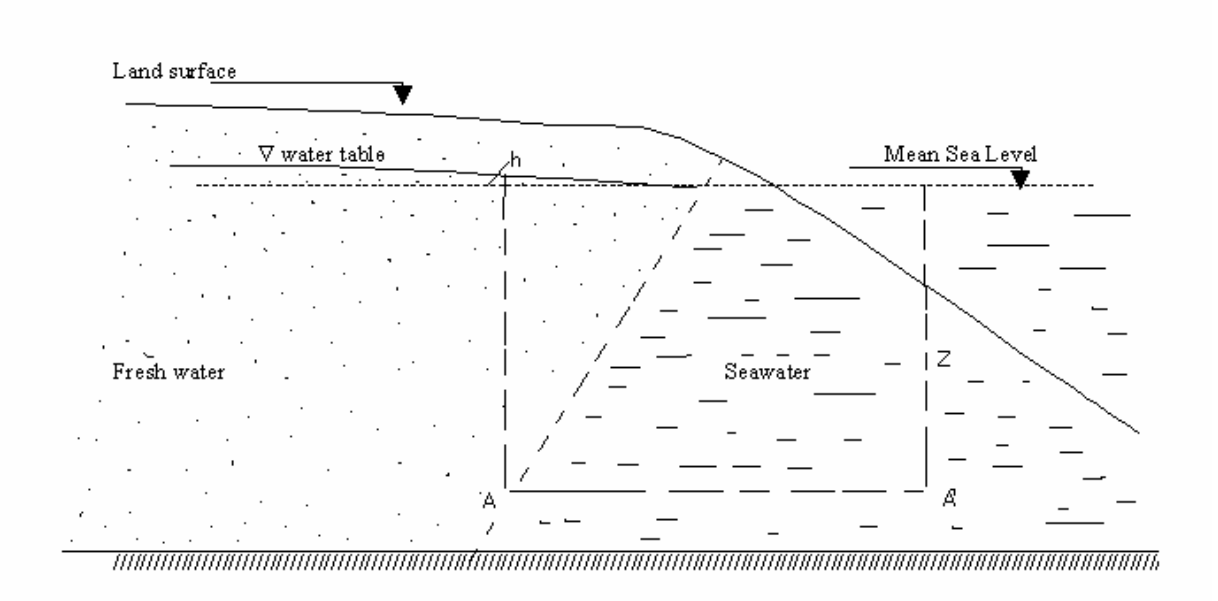

Figure 3.1 Explanation Badon Ghyben-Herzberg Principle in an idealized hydrostatic fresh-salt groundwater system (Bruggeman et al. 1987).

Freshwater pressure at point A $P_A = (h_f + z) * \rho_f$ (3.1)

Saltwater pressure at point A' $P_{A'} = z * \rho_s$ (3.2)

h_f = freshwater head (water table elevation over mean sea level)

z = depth to the interface below mean sea level

ρ_f = freshwater density = 1000 kg/m^3

ρ_s = saltwater density = 1025 kg/m^3

$\alpha = \rho_f / (\rho_s - \rho_f)$ (3.3)

α is the ratio of fresh water density to the density difference of fresh and saline water.

On the interface $\rho_A = P_{A'}$, hence, depth to the interface below mean sea level is expressed as:

$$z = \frac{\rho_f}{(\rho_S - \rho_f)} h_f = \alpha h_f \tag{3.4}$$

Which is the well known Badon Ghyben-Herzberg Formula.

The major shortcomings of this approach are as follows: (1) The position of the interface is directly related only to the head of the water table, (2) There is no vertical head gradient, and (3) Freshwater occurs in a single point at the coastline that is it will vanish at the coastline (Kooi and Groen, 2001).

3.1.2. Stating the Dynamics of the System

Hubbert (1940) changed the first assumption (mentioned above) of Ghyben-Herzberg by relating the interface position to both freshwater head and saltwater head:

$$z = \frac{\rho_f}{(\rho_f - \rho_s)} h_f - \frac{\rho_s}{(\rho_f - \rho_s)} h_s \tag{3.5}$$

Where z is now vertical location above datum of a point on the interface and h_f is freshwater head and h_s is saltwater head. The above formula defines the position of the interface under equilibrium conditions that is when the saltwater is stationary or when both fluids are in motion. Therefore, apart from consideration of the saltwater head in the formula, Hubbert (1940)

together with Mustak (1937) were partially accounted for the dynamics of the system.

Moreover, Bear and others also contributed to quantification and understanding of saltwater-freshwater dynamics (Bear and Tod, 1960). Bear and Dagan (1964) first investigated the analysis of transient movement of interfaces, although Henry (1962) also investigated transitory movement in a more approximate large-scale system.

3.1.3. Horizontal Seepage Face

Glover (1959) and Edelman (1972) relaxed the third assumption, allowing a horizontal seepage face to develop in the offshore (Figure 3.2).

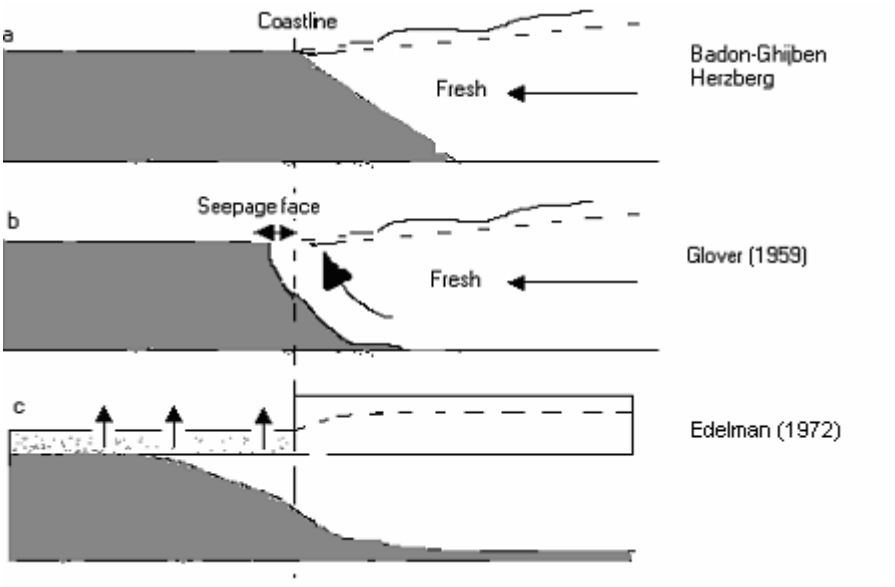

Figure 3.2. Schematic illustration of subsurface lithological conditions and the geometry of the interface/transition zone between fresh and salt water in coastal areas for a number of classical studies (modified from Kooi and Groen (2001).

Glover (1959) developed a formula, which accounts for the movement and discharge of the freshwater.

$$\gamma^2 - \frac{2Q}{\gamma} X - \frac{Q^2}{\gamma^2 K^2} = 0 \qquad (3.6)$$

Where Q is fresh water flow per unit length of shore (L^2T^{-1}), K is hydraulic conductivity flow of the medium (LT^{-1}), $\gamma = (\rho_s - \rho_f) / \rho_f$ (dimensionless), ρ_s is density of saltwater (ML^{-3}), ρ_f is density of saltwater (ML^{-3}), X is distance from shore (L) and Y is depth from mean sea level (L).

3.1.4. Introduction of Dispersion Zone

Cooper (1959) developed a qualitative hypothesis to explain the mixing (or zone of dispersion) and the associated perpetual circulation of seawater observed in the various field investigation. Henry (1959) also developed some solutions for determining the sharp interface under various conditions and made the first attempt to quantitatively determine the effects of dispersion and density dependent fluid flow on saltwater encroachment in coastal aquifers (Henry, 1964). He corroborated Cooper's hypothesis and opened a new approach using the advection-diffusion equation (miscible fluids) instead of sharp interface (immiscible fluids) approach.

3.1.5 Application of Fluid Density Dependent Flow In Seawater Intrusion

Usually flow and transport are modeled separately, in this case it is assumed that the density of the fluid is constant. Although this is the case in most of

the problems, there are cases where density variation in the domain and with time cannot be neglected.

In situations where constant density is assumed, the flow has influence on the contaminant transport particularly in the absence of other factors participating in the solute transport. The velocity of groundwater is enough to transport any contaminant in the advection process. Moreover, if the other factors are considered operating in the transport processes (geometry of the media, longitudinal and transversal dispersivity, and solute interaction to the media) rather than just a groundwater velocity still groundwater flow can be simulated separately then in the next step the effect of other factors are considered on the solute transport.

However, the distribution of a transport variable may affect flow, if one of the relevant parameters depends on that variable. In other words, the dissolved substance in the groundwater has property variation that can affect the groundwater flow pattern. Important parameters are fluid properties and the most important of these is the density of the fluid. If there is density gradient in the system, flow would generally not be the same as in a constant-density situation. Here coupling of fluid flow and transport simulation becomes necessary.

The solute transport is more general treatment, in that saline and freshwaters mix producing a continuous variation of the concentration. In general, this approach requires simultaneous solution of the groundwater equation and the advection-diffusion transport equation because density is a function of concentration. Voss (1984) used this approach and developed a finite element simulation model for saturated-unsaturated, fluid-density-dependent groundwater flow with energy transport or chemically reactive single species solute transport under the code of SUTRA. The SUTRA code was used for the modeling of seawater intrusion in the Selçuk sub-basin together

with the Argus One (Open Numerical Environment) graphical user interface (GUI). In the following sections, density dependent saturated groundwater flow and solute transport equations used by the SUTRA and related parameters are introduced from Voss (1984).

3.2. Fluid Physical Properties

The groundwater fluid density and viscosity may vary depending on pressure and solute concentration. These fundamental variables are defined as follows:

P	$\|M/(L.S^2)\|$	fluid pressure
C	$\| M_s/M\|$	fluid solute mass fraction

(or solute concentration, mass solute per mass total fluid)

The concentration and pressure are the main variables acting in the solute transport process. Here the fluid concentration is expressed as mass fraction, and do not correspond to 'solute volumetric concentration', which is defined in terms of fluid density.

Fluid density, ρ M/L_f^3 while a weak function of pressure is primarily dependent upon fluid solute concentration and temperature.

$$\rho = \rho(C) \approx \rho_o + \frac{\partial \rho}{\partial C}(C - C_o) \qquad (3.7)$$

ρ_o	$[M/L_f^3]$	base fluid density
C_o	$[M_s/M]$	base fluid solute concentration at ρ_o

The factor $\frac{\partial \rho}{\partial C}$ is a constant value of density change with concentration. For mixtures of fresh and sea water at 20 ^{o}C, when C is the mass fraction of total dissolved solids, C_o = 0, and ρ_o = 998.2 [kg/m^3], then the factor is approximately 700. [kg/m^3].

Fluid viscosity, μ [M/L$_f$s], is a weak function of pressure and of concentration, and depends primarily on fluid temperature. For solute transport, viscosity is taken to be constant. At 20 ^{o}C in m-k-s units:

$$\mu(C)|_T = 20\,^{o}\text{C} = 1.0 \times 10^{-3} \ \text{[kg/(m.s)]} \qquad (3.8)$$

3.3. Properties of Fluid within the Solid Matrix

ε: porosity (volume of voids per total volume)

The specific pressure storativity, S_{op}, is expressed as:

$$S_{op} = (1-\varepsilon)\alpha + \varepsilon\beta \qquad (3.9)$$

Where β is a fluid compressibility and α is solid matrix compressibility. Note that the common specific storage, S_o [L^{-1}], $S_o = \rho\,|g|\,S_{op}$, where |g| [l/s^2] is the magnitude of the gravitational acceleration vector. When S_o is multiplied by confined aquifer thickness gives the well known storage coefficient, S. Water compressibility is 4.47x10^{-10} 1/kg/ms^2. Solid matrix compressibility ranges are 10^{-8}-10^{-10}, 10^{-6}-10^{-8}, 10^{-7}-10^{-9}, 10^{-8}-10^{-10} m^2/N for jointed rock, clay, sand, and gravel, respectively (Freeze and Cherry, 1979).

3.4. Fluid Mass Balance

Net outflow rate per unit volume equals the time rate of change of fluid mass per unit volume.

$$-\nabla \rho q = \frac{\partial(\varepsilon\rho)}{\partial t} \tag{3.10}$$

Where the term on the right hand side represents the rate of change of mass of the fluid per unit volume of porous medium.

Since flux, q = ε ν, the equation 3.12 becomes:

$$-\nabla(\rho\varepsilon v) = \frac{\partial(\varepsilon\rho)}{\partial t} \tag{3.11}$$

Average fluid velocity ν [L/s] in equation 3.13 can be expressed using Darcy's law as

$$v = -\left[\frac{k}{\varepsilon\mu}\right](\nabla p - \rho g) \tag{3.12}$$

where

k	[L^2]	solid matrix permeability
g	[L/s^2]	gravitational acceleration (gravity vector)

Substituting equation 3.12 into equation 3.11:

$$\nabla\left[\frac{k\rho}{\mu}\right](\nabla p - \rho g) = \frac{\partial(\varepsilon\rho)}{\partial t} \tag{3.13}$$

Opening partial differential term in equation 3.13, following the fluid mass balance equation for transient state can be obtained :

$$\nabla\left(\frac{k\rho}{\mu}\right)(\nabla p-\rho g)=(\rho S_{OP})\frac{\partial p}{\partial t}+\varepsilon\left(\frac{\partial \rho}{\partial C}\right)\left(\frac{\partial C}{\partial t}\right) \tag{3.14}$$

This equation describes density-dependent groundwater flow in saturated porous medium.

3.5. Solute Mass Balance

Solute mass is transported through the porous media by flow of groundwater (solute advection) and by molecular or ionic diffusion, which is small at field scale. In addition, the actual groundwater flow may vary from the average groundwater flow calculated from the Darcy's law. This may cause mixing of groundwater with different concentrations moving both faster and slower than that of the average velocity.

Solute transport simulation accounts for a single species mass stored in fluid solution as solute. Because solute considered in this study is chloride which is none reactive species, no adsorbate interaction should be considered. Mass balance of solute can be stated as mass out flow per unit volume equals the time rate of change of mass within the unit volume.

$$-\nabla J=\frac{\partial(C\varepsilon\rho)}{\partial t} \tag{3.15}$$

Where mass flux, J, can be expressed by means of advective flux,

$$\nabla Jadv=\nabla(\varepsilon\rho vC) \tag{3.16}$$

and diffusive flux,

$$-\nabla Jdif = \nabla(\varepsilon\rho(Dm + D)\nabla C) \tag{3.17}$$

where:

D is dispersion tensor and Dm is apparent molecular diffusivity of solute in solution in porous media including tortuosity effects.

For the non-reactive and non-adsorbate case, solute mass balance can be stated by substituting equation 3.16 and 3.17 into 3.15 as:

$$-\nabla(\varepsilon\rho vC) + \nabla(\varepsilon\rho(D_m + D)\nabla C) = \frac{\partial(C\varepsilon\rho)}{\partial t} \tag{3.18}$$

This equation describes time rate change of concentration as a function of advective and diffusive mass fluxes together with dispersion effect in porous medium within a given unit volume.

CHAPTER 4

STEADY STATE AREAL SATURATED FLOW SIMULATIONS

Density dependent cross sectional modeling, which will be used to simulate seawater-fresh groundwater relationships in the Selçuk sub-basin aquifers, requires pre-pumping period (steady state) head data for the groundwater level calibration. However, no data exist for the Selçuk sub-basin plain area through mid-point of which the cross-section will be taken. In order to obtain steady state head values for the plain area, steady state two dimensional density independent areal saturated flow model simulation was performed and calibrated against available monitoring data of the wells (18495 and 21381) located along the sides of the plain.

4.1. Conceptual Model

The domain of the model covers plain area of the sub-basin as shown in Figure 4.1. The Marble, Neogene, and Alluvium units in this plain area are treated as a single aquifer having different hydrogeological characteristics. Thickness of the aquifer is 200 m (thickness of the Alluvium plus the Neogene units as determined from the well logs of 54131 and 54132) and plus the topographic elevation at a given location. The aquifer is subject to precipitation recharge in the domain area. Along the North-Northeastern side, influx occurs from the Bayındır-Torbalı sub-basin. Additional influx into the aquifer takes place from the permeable marble units composing

highlands at east. There is no flow relation between the modeled aquifer and the impermeable marble units composing highlands along the Northern and southern boundary of the domain. It is also assumed that no flow relationship exists between the Küçük Menderes River and the aquifer modeled.

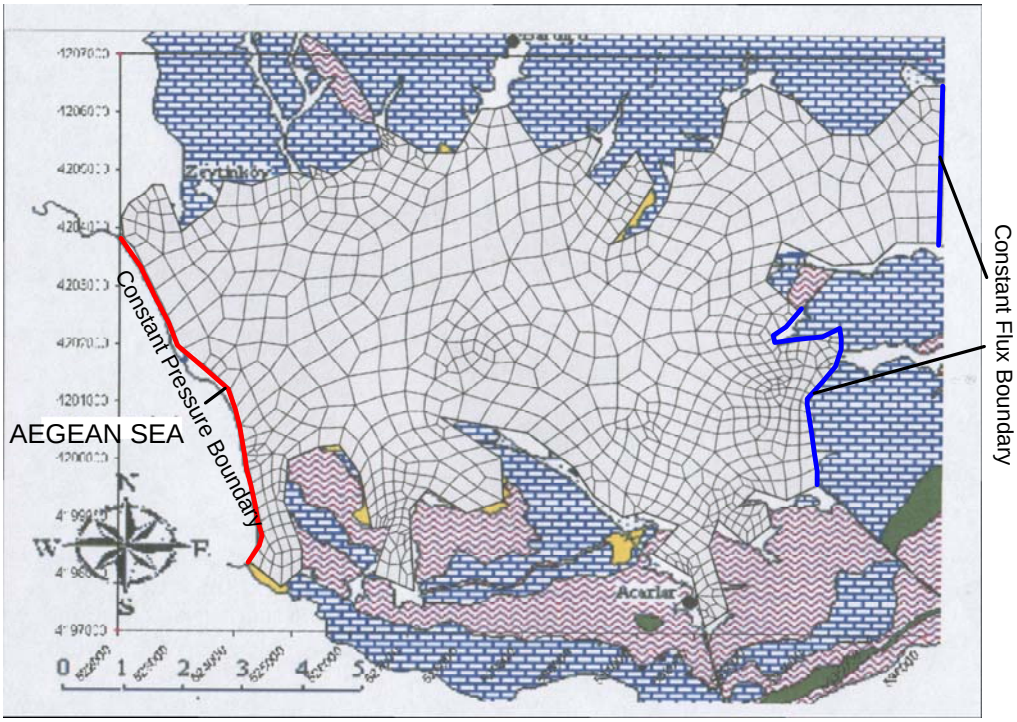

Figure 4.1 Boundary conditions and mesh system applied to the areal domain.

4.2. Discretization of the Domain and Boundary and Initial Conditions

The irregular finite element mesh is created in the domain and is used during simulations (Figure 4.1). Number of elements and number of nodes present in the mesh are 846 and 992, respectively.

Three types of flow boundary conditions are used in the model: (1) Constant, zero, pressure boundary which is assigned along the western boundary of the sub-basin where shore line is present (Figure 4.1), (2) Constant flux boundary which is assigned to the eastern boundary representing the recharge from the Bayındır-Torbalı sub-basin and to the marbles at east representing the recharge from the highlands (Figure 4.1), (3) No flow boundary which is assumed to exist along northern and southern boundaries. Zero pressure is assigned as initial pressure condition to whole domain.

4.3. Parameters

Permeability, porosity and recharge values assigned to the aquifer are listed in Table 4.1. Net plain area recharge value of Gündoğdu (2000) is converted to kg/s per unit area and assigned to the plain model domain after considering the total modeled plain area as precipitation recharge value. The total recharge area is automatically calculated by the SUTRA-GUI software once contoured. Similarly, recharge from the eastern marbles was calculated from the highland recharge data of Gündoğdu (2000). But this time, converted recharge was assigned as flux (subsurface recharge). Discharge calculated by Yazicigil et al (2000a) from the Bayındır-Torbalı sub-basin is used as recharge to the Selçuk sub-basin. Total recharge (269.7 kg/s) considered for the model domain is in agreement with the recharge (253.8 kg/s) estimated by DSI (1973).

Table 4.1 Parameters used in the areal model.

Parameter	Value	Unit
Permeability of Alluvium	$0.08 \times 10^{-11} - 1.7 \times 10^{-11}$	m^2
Permeability of Neogene	$0.24 \times 10^{-11} - 2.4 \times 10^{-11}$	m^2
Permeability of Marble	$0.11 \times 10^{-11} - 4.00 \times 10^{-9}$	m^2
Porosity	20	%
Total recharge	269.7	Kg/s

4.4. Calibration and Results

Calibration of a flow model refers to the demonstration that the model is capable of producing field measured heads. To calibrate the steady state pressure distribution, the observation well data of 18495 and 21381 (average of 1976-1977) were used. Calibration results are shown in Table 4.2. On the bases of simulated and observed pressure difference, it could be concluded that the model is successfully calibrated.

Table 4.2. Observed and simulated groundwater levels and pressures of the steady state areal model calibration.

Well no	Observed head (m)	Simulated head (m)	Residual head (m)
18495	1.84	1.94	0.10
21381	1.82	1.77	0.05

Well no	Observed Pressure ($kg/m.s^2$)	Simulated Pressure ($kg/m.s^2$)	Residual Pressure ($kg/m.s^2$)
18495	18032	19012	980
21381	17836	17346	490

Steady state groundwater pressure map prepared using the calibration results is shown in Figure 4.2 where the cross-section line used for the cross-sectional density dependent flow and solute transport modeling, presented in the next chapter is also indicated.

The cross-section extends from the shoreline of the Agean Sea at southwest to northeast toward Belevi. Moreover the cross-section passes through well no: 54131.

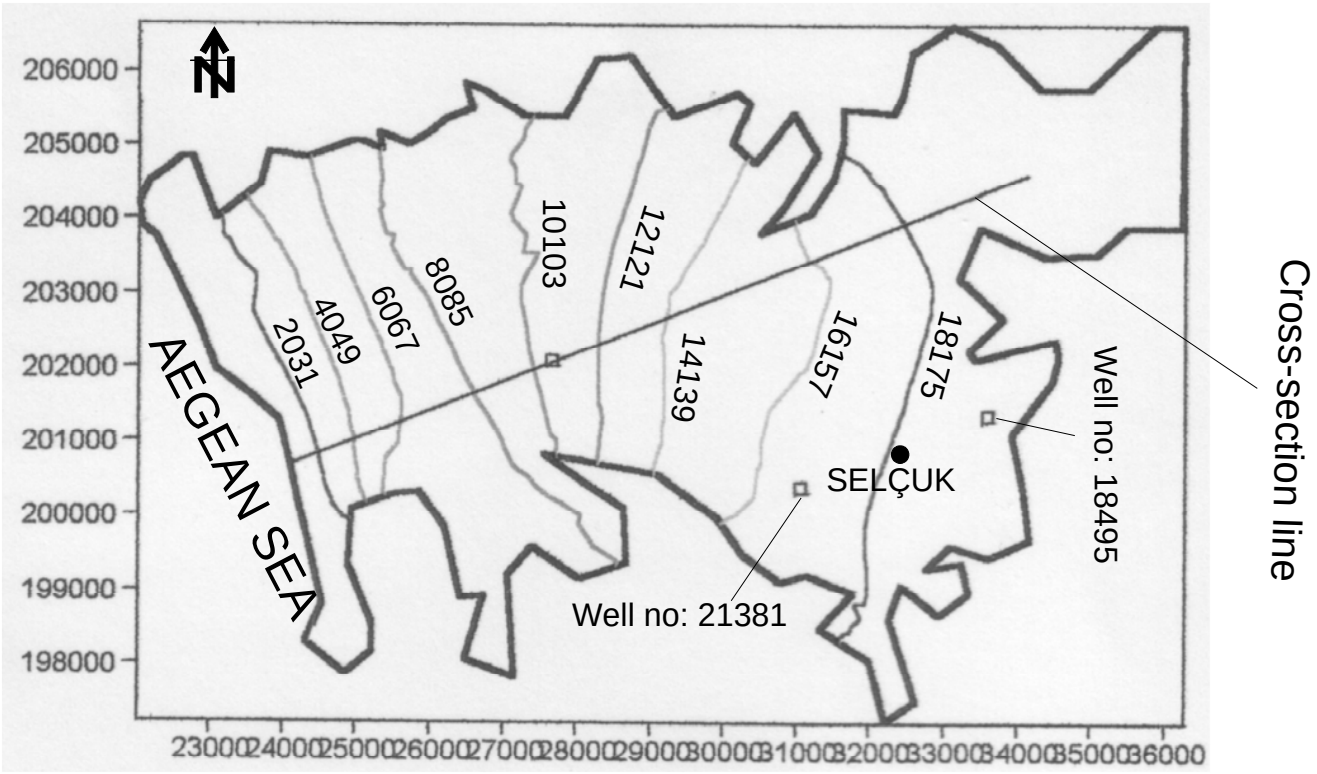

Figure 4.2 Steady state groundwater pressure (kg/m.s^2) distribution.

CHAPTER 5

DENSITY DEPENDENT CROSS SECTIONAL SATURATED FLOW AND SOLUTE SIMULATIONS

Southwest-Northeast cross section is selected to simulate the seawater intrusion in the area (Figure 4.2). Cross sectional simulations are composed of two phases as pre-pumping period, representing pre-1975 and post-pumping period, representing 1975-2002 period.

5.1. Conceptual Model

The domain of the model covers a cross-sectional area taken from the middle section of the plain along SW-NE direction. Horizontal extent of the domain covers 11000 m from shoreline to landward (Figure 5.1). The model domain is composed of the Alluvium and the Neogene units, which are treated as a single aquifer having similar hydrogeological characteristics as suggested by the well log data of 54131 and 54132. Vertical cross-sectional extent of the model domain is taken as 200 m with respect to sea level. 200 m thickness of the Alluvium plus Neogene units in the plain is determined from the well logs of 54131 and 54132. Lateral extent of the cross-section is the width of the plain area.

The aquifer is subject to recharge through precipitation from the top section of the domain. The recharge area divided into four segments in order to substract discharge values from the recharge of relevant segments during

post-pumping period later on. In other words, discharge at a given transient period was substracted from recharge value at corresponding segment. The Segment I extends from shoreline to the discharge wells (about 6000 m) where Cooperative II wells are present. The Segment II covers the Cooperative II discharge well locations about 900 m and starts from the end of Segment I. The Segment III covers the discharge well locations (about 700 m) where Cooperative I wells are present and starts from the end of Segment II. The Segment IV extends from cooperate I wells to the end of cross-sectional line at right. The other recharge area present along the right vertical boundary of the model domain representing influx from the Bayındır-Torbalı sub-basin aquifer. No flow occurs along the bottom boundary.

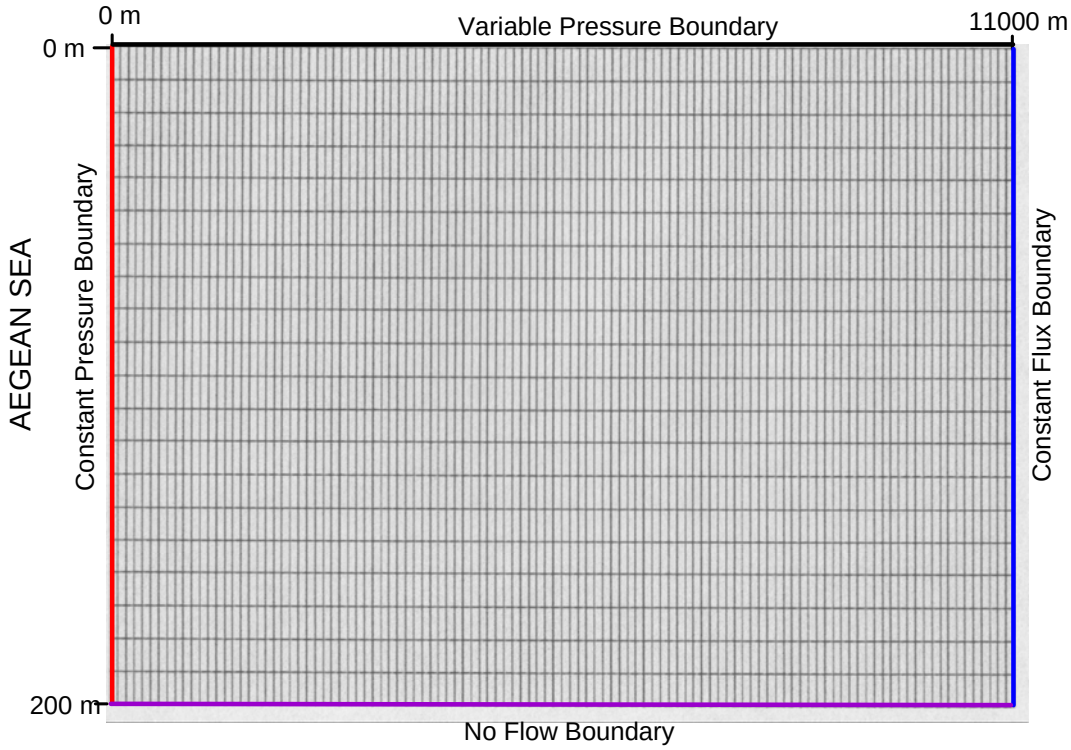

Figure 5.1 Boundary conditions and mesh system applied to the cross sectional model domain.

5.2. Discretization of the Domain and Boundary and Initial Conditions

Fishnet mesh of 110 m x 20 m elements was used for the cross sectional model (Figure 5.1). The mesh is composed 2200 elements and 2331 nodes. Total length of the model domain along x- (horizontal) direction is taken as 11000 m. Total thickness of the model domain along y- (vertical) direction is 200 m which is based on the thickness information of alluvium and Neogene units determined from well log of 54131 and 54132.

Four types of flow boundary conditions were used in the cross sectional model: (1) Constant hydrostatic pressure boundary that is assigned along the left vertical boundary where shoreline is present (Figure 5.1). During hydrostatic pressure calculations, chloride concentration dependency of the density is also taken into account, (2) Constant flux boundary which is assigned along the right vertical boundary representing the recharge from the Bayındır-Torbalı sub-basin as shown in Figure 5.1, (3) No flow boundary is assigned along the bottom of the domain, and (4) Variable pressure boundary is applied to the upper section of the domain.

During pre-pumping period (steady state) runs, hydrostatic pressure calculated using seawater properties is assigned as initial pressure condition. Initial concentration is assumed to be 0.0225 [kg (dissolved solid)/ kg (seawater)] of the Aegean seawater representing the regressed sea condition.

Pre-pumping period pressure and concentration calibration results were later used as initial pressure and concentration values in the beginning of the post-pumping calibration runs.

5.3. Parameters

Permeability, porosity, recharge, water compressibility, solid matrix compressibility, molecular diffusion coefficient and dispersivity values used in the model are listed in Table 5.1. The value of solid matrix compressibility is so chosen that the value of specific yield becomes about 0.1 as suggested by the well data. Molecular diffusion coefficient of Cl in fluid is determined from the literature (Rowe et al., 1988, Baron et al., 1989, Voss and Andersson, 1993). The parameters governing magnitude of dispersion were fixed at the minimum possible value that gives stable solutions to the transport equation for the mesh used. The values were taken from Domenico and Schwartz (1999). The total recharge in Table 5.1 represents the sum of precipitation recharge and the Bayındır-Torbalı sub-basin recharge to the Selçuk sub-basin.

Table 5.1 Parameters used in the cross sectional model

Parameter	Value	Unit
Permeability	$0.08x10^{-11} – 1.0x^{-10}$	m^2
Porosity	20	%
Total recharge	80.87	kg/s
Molecular diffusion coefficient of Cl in fluid	$7.0x^{-10}$	kg/m^3
Dispersivity (longitudinal)	15	m
Dispersivity (transverse)	1.5	m
Water compressibility	$4.47x10^{-10}$	$1/kg/ms^2$
Solid matrix compressibility	$7.0x^{-8}$	m^2/N

The discharge values based on irrigation and domestic needs were determined for the post-pumping period runs and are summarized in Table 5.2. Domestic need discharge for a given period was approximated using population versus discharge relationship equation [Municipality discharge (Kg/s) = 0.0035 * population] based on 1997 population and municipality discharge data.

Table 5.2 Discharge values used in the post-pumping period cross sectional runs.

Total average discharge (kg/s)	Period
-42	1976 - 1977
-88	1978 - 1988
-143	1989 -1990
-157	1991 - October, 2001
-4.6	November, 2001 - May, 2002

5.4. Calibration and Results

5.4. 1. Pre-pumping Period

The pre-pumping period calibration was performed in order to obtain steady state pressure values along the cross-section line which were estimated during the areal model simulations. The calibration runs were performed as trasient runs but because recharge values are not changed and no discharge is introduced during pre-pumping period run, system behaves like steady state. The pre-pumping calibration runs were carried out for 1000 years with

1 month time increment using 100 year output option. It is observed that pressure values practically do not change after about 100 years. In these runs, observed (estimated from the areal simulation) versus calculated pressure comparisons were performed by calibrating permeability and recharge values. Comparison of the observed (estimated from areal simulation) and calculated final pressures is shown in Figure 5.2.

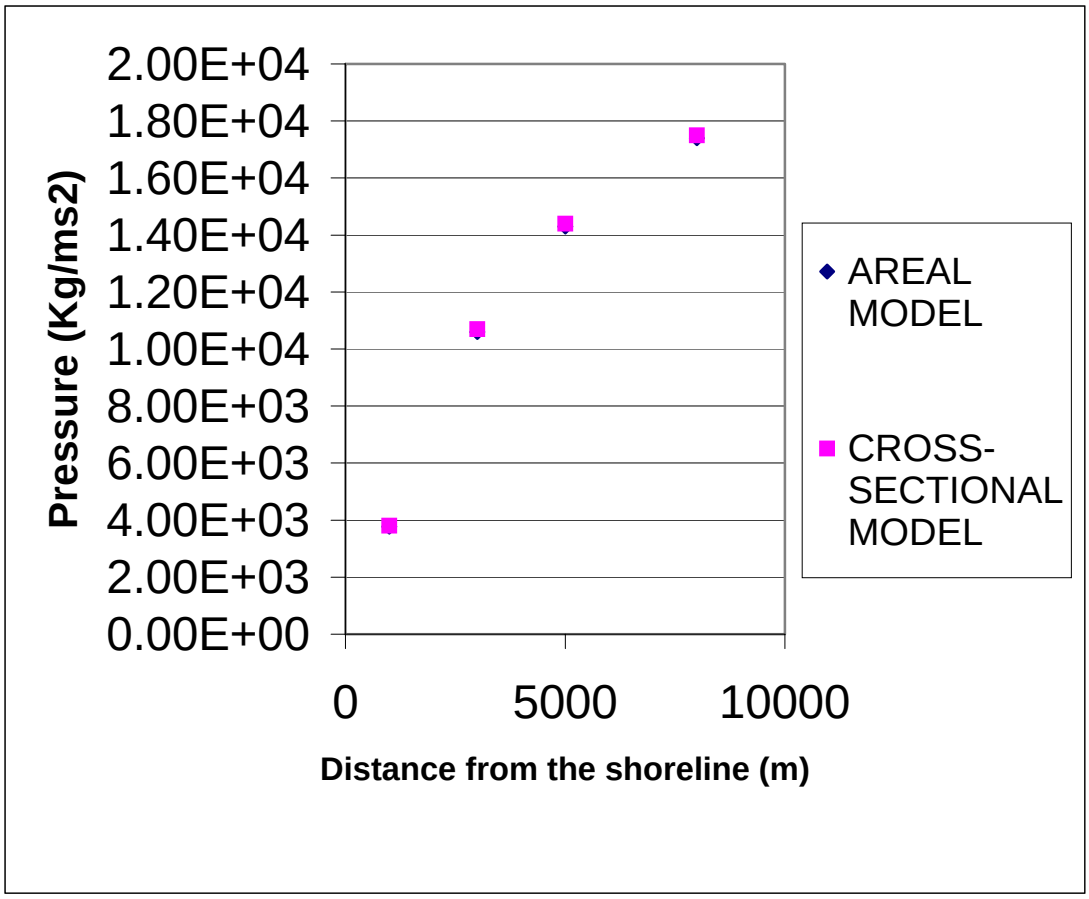

Figure 5.2 Comparison of estimated pressure (from areal simulation) versus calculated pressure values obtained from the pre-pumping cross sectional model.

Because pre-pumping period chloride concentration data for the aquifer are not available, no calibration is performed related to the concentration transport parameters (dispersivity, molecular diffusion coefficient) during pre-pumping simulations. Concentration calibration is carried out later during post-pumping period runs. During pre-pumping runs, it is observed that for calibrated values (as determined after post-pumping calibration runs), seawater protrusion takes place and the interface reaches a steady state after about 600 years. Pre-pumping period chloride distribution in the aquifer at the end of 600 years is shown in Figure 5.3. In the figure, the perpendicular line at about 4200 m represents the location of well 54131 and 54132. Selçuk town corresponds to about 7000 m on the figure at the south of the cross section line.

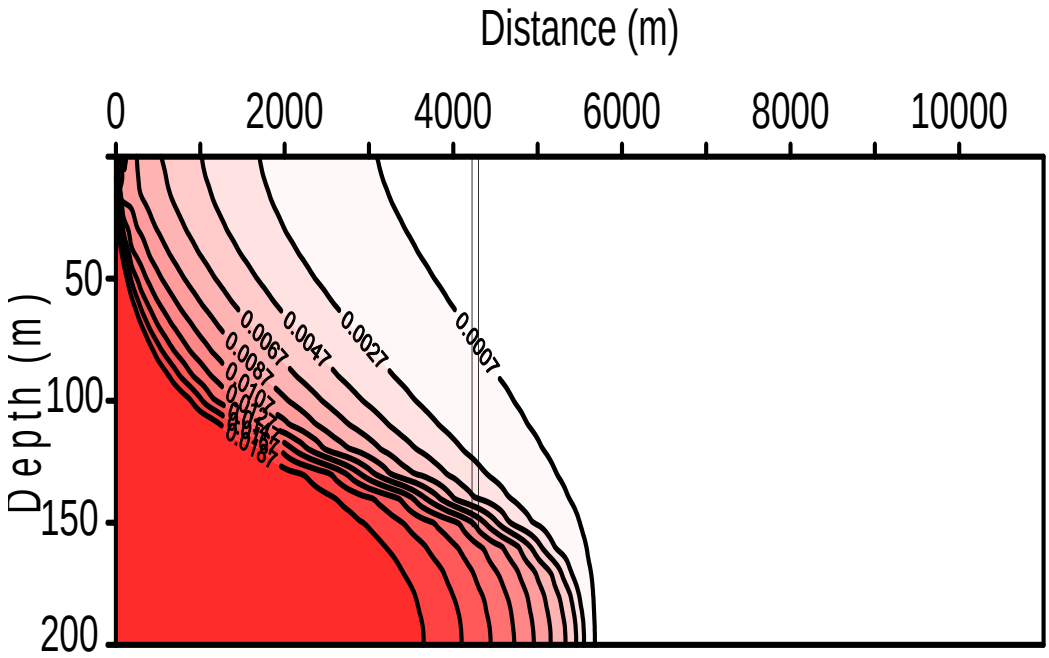

Figure 5.3 Pre-pumping period chloride concentration (kg/kg) distribution in the aquifer.

5.4. 2. Post-pumping Period

Chloride transport and storativity values were calibrated during post-pumping period runs. The post-pumping runs were carried out in monthly increments by taking into account of changing discharge conditions in the sub-basin between the years of 1975 and 2002.

After the calibration, observed versus calculated pressure values at May 2002 at well location of 54131 (only monitoring well in the plain area) is equal to 1.22×10^4 and 1.07×10^4, respectively. Chloride concentrations measured at depths of 65 m, 110 m and 140 m in May, 2002 are compared with the observed values in Table 5.3. Chloride concentration distribution estimated from May 2002 EC data at well location of 54131 is compared with the post-pumping period May, 2002 results in Figure 5.4. As it can be seen from the table and the figure, salt water interface in the area is reasonably well predicted after the post-pumping period simulations. Chloride concentration distribution in the aquifer by the end of post-pumping period is shown in Figure 5.5.

Table 5.3 Measured and simulated chloride concentrations in well water of 54131 in May 2002.

Depth (m)	Observed concentration (kg/kg)	Simulated concentration (kg/kg)
65	8.55×10^{-4}	4.47×10^{-4}
110	8.03×10^{-3}	7.83×10^{-3}
140	1.55×10^{-2}	1.29×10^{-2}

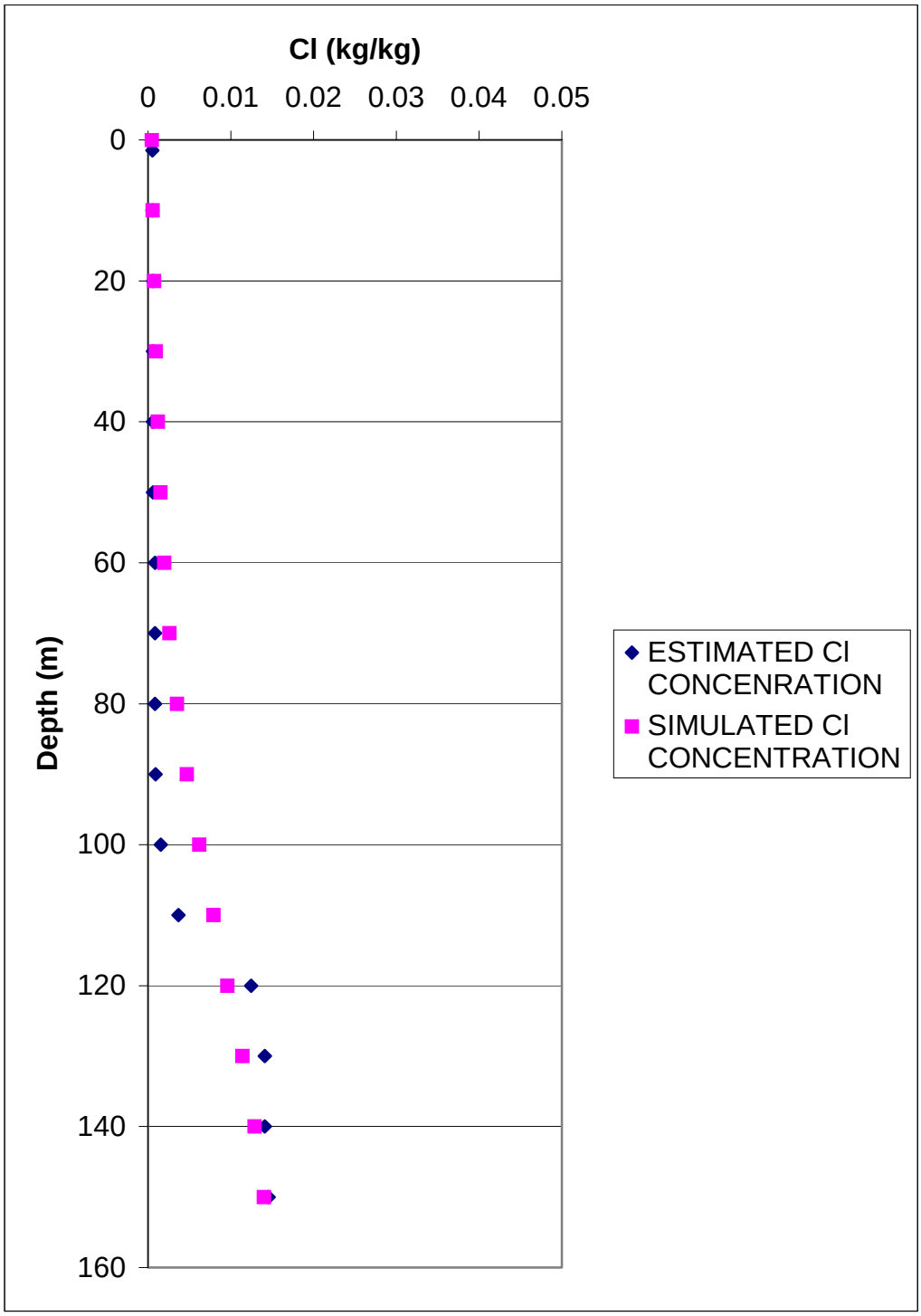

Figure 5.4 Comparison of observed (estimated from EC data) versus calculated chloride concentration in May, 2002 at the location of well 54131.

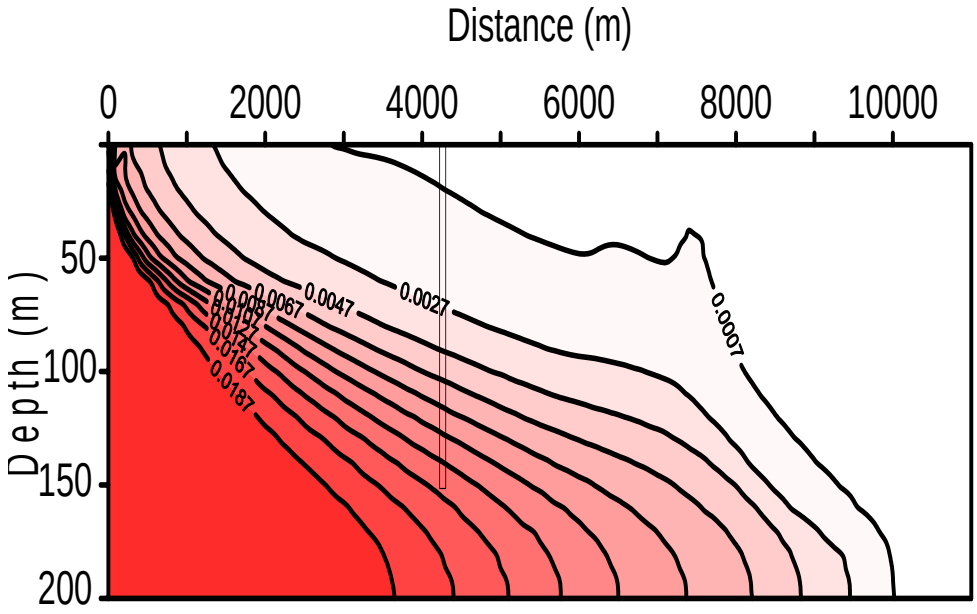

Figure 5.5 Chloride concentration (kg/kg) distribution in the aquifer at present (at the end of post-pumping period).

The post-pumping period simulations indicate that present pumping conditions in the Selçuk sub-basin have caused seawater intrusion. The shape of the concentration contours indicate an upconing problem where Selçuk town is present at the south of the cross section line (Figure 5.5).

CHAPTER 6

PREDICTION SIMULATIONS

Five scenarios are simulated for future predictions: (1) Present recharge and discharge conditions are maintained, (2) Discharge increases at a rate of the municipality need as a result of increasing population, (3) Discharge decreases by 12% from the present value, (4) Discharge decreases by 25% from the present value, and (5) No discharge occurs or recharge amount equals to the present discharge amount conditions occur in the aquifer.

6.1. Scenario One

In this scenario, present recharge and discharge conditions are maintained and the simulation was carried out for 20 years, starting from 2002. Simulated head values suggest that present groundwater levels would decrease about 0.24 m on the average between 6000 m and 8000 m from the shoreline with respect to present level. Chloride concentration distribution obtained at the end of Scenario I is shown in Figure 6.1. Chloride concentration would increase about 140% (from present 0.00073 kg/kg to 0.00178 kg/kg) at a depth of 50 m and increase about 85% (from present 0.00322 kg/kg to 0.00592 kg/kg) at a depth of 100 m at the distance of 6000 m from the shoreline.

The above scenario indicates that if the present discharge conditions continue without any management measures, water of present pumping wells (recovering water from a depth range of about 40-80 m with respect to

sea level) would be degraded due to upconing in the following years, in other words the upconed poor quality water migrate further to the upper portion of the aquifer (Figure 6.1).

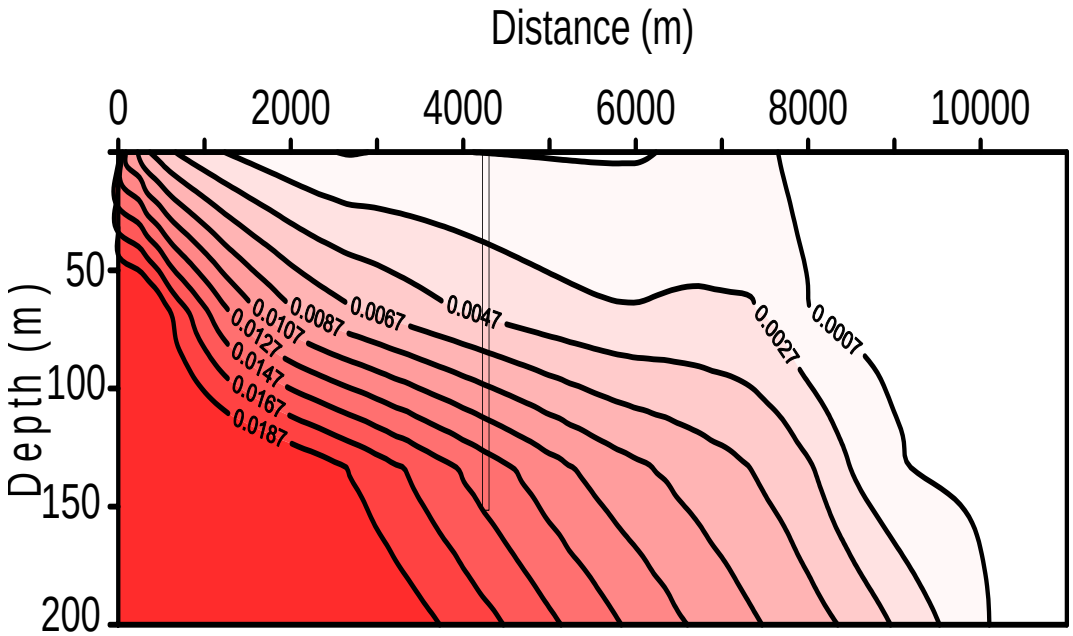

Figure 6.1 Chloride concentration (kg/kg) distribution in the aquifer in the year of 2022 under Scenario I conditions.

6.2. Scenario Two

In this scenario, discharge increases at a rate of the municipality need as a result of increasing population in the next 20 years. Discharge increase is about 15% (30 kg/s) on the average. Simulated head values indicate that groundwater levels would decrease of about 0.25 m on the average between 6000 m and 8000 m from the shoreline with respect to present levels. Chloride concentration distribution in the aquifer at the end of Scenario II is

shown in Figure 6.2. Chloride concentration would increase about 160% (from present 0.00073 kg/kg to 0.00190 kg/kg) at a depth of 50 m and increase about 87% (from present 0.00322 kg/kg to 0.00603 kg/kg) at a depth of 100 m at distance of 6000 m from the shoreline. The upconing is slightly greater in the results of this scenario than those of Scenario I. In both cases, however, water of present wells in the area would have chloride concentrations greater than the permissible irrigation limit of 0.0007 kg/kg.

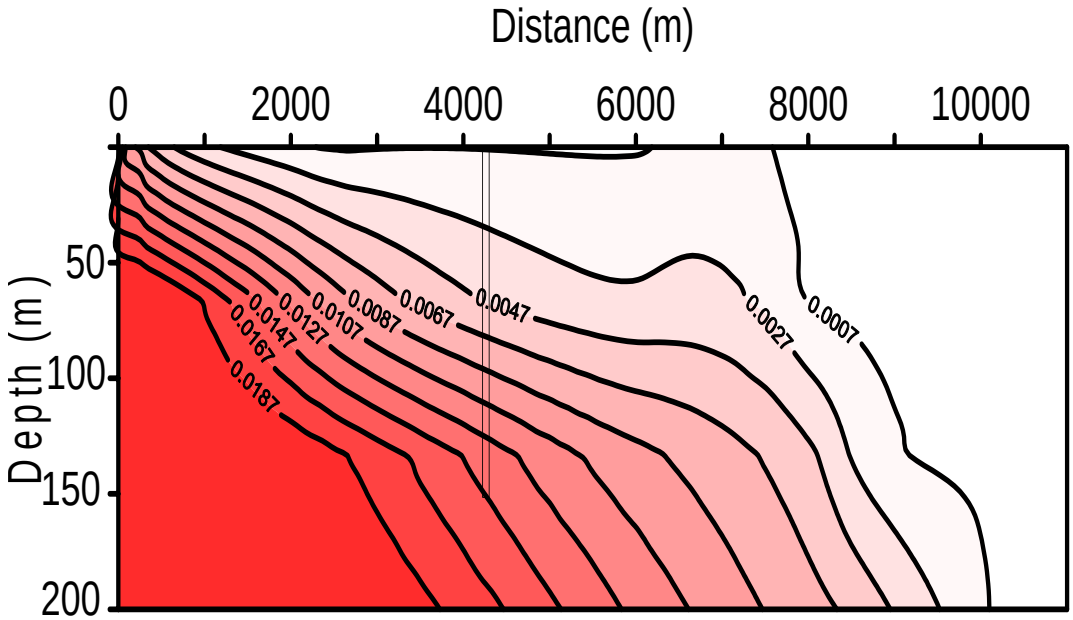

Figure 6.2 Chloride concentration (kg/kg) distribution in the aquifer in the year of 2022 under Scenario II conditions.

6.3. Scenario Three

In this scenario, present discharge decreases by 12% (about 18 kg/s) on the average in the next 20 years. Simulated head values indicate that groundwater would increase about 0.07 m from present levels on the

average between 6000 m and 8000 m from the shoreline. Chloride concentration distribution in the aquifer at the end of Scenario III is shown in Figure 6.3. Chloride concentration increases about 94% (from present 0.00073 kg/kg to 0.001416 kg/kg) at a depth of 50 m and increases about 69% (from present 0.00322 kg/kg to 0.00544 kg/kg) at a depth of 100 m at distance of 6000 m from the shoreline although discharge was decreased by 12%. The upconing continues but it is less than that of Scenario I and II.

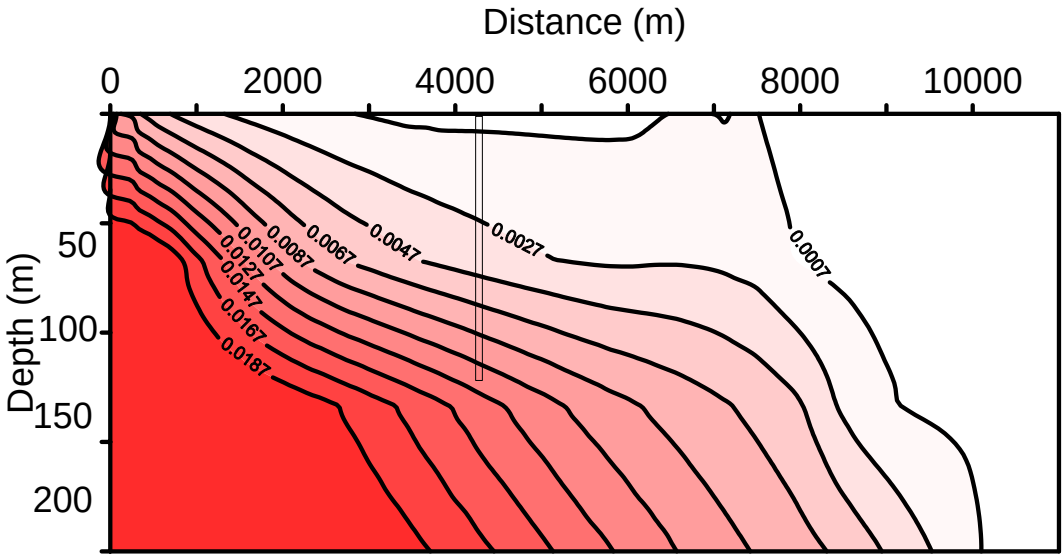

Figure 6.3 Chloride concentration (kg/kg) distribution in the aquifer in the year of 2022 under Scenario III conditions.

6.4. Scenario Four

In this scenario, present discharge decreases by 25% (about 37kg/s) on the average in the next 20 years. The simulated head values suggest that groundwater levels would increase about 0.08 m on the average between 6000 m and 8000 m from the shoreline. Chloride concentration distribution

obtained at the end of Scenario IV is shown in Figure 6.4. Chloride concentration increases about 69% (from present 0.00073 kg/kg to 0.001235 kg/kg) at a depth of 50 m and increases about 61% (from present 0.00322 kg/kg to 0.00519 kg/kg) at a depth of 100 m at distance of 6000 m from the shoreline. Although discharge decreased by 25%, the upconing continues.

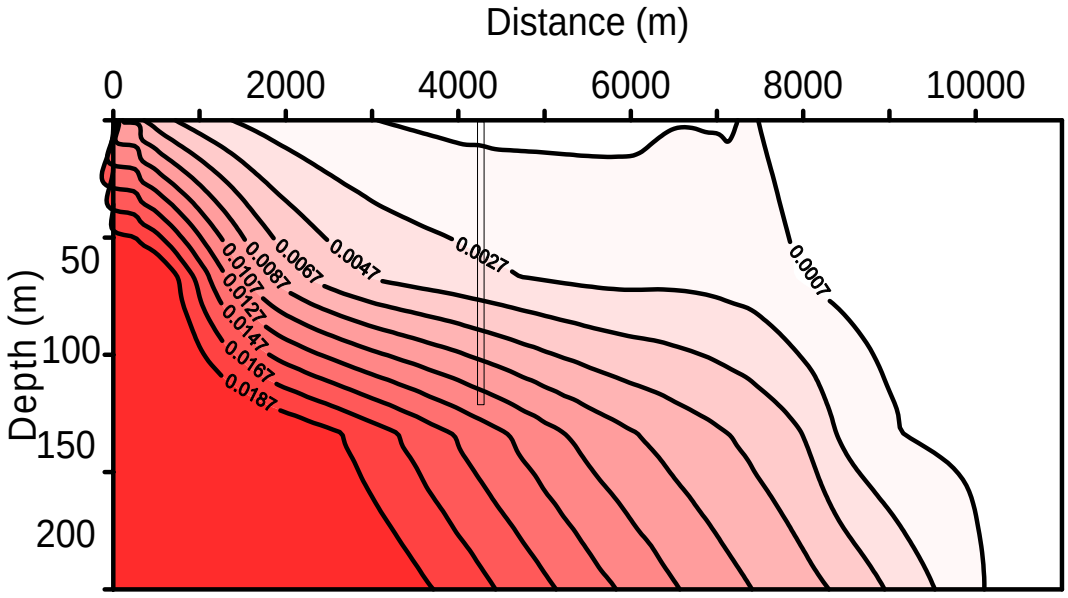

Figure 6.4 Chloride concentration (kg/kg) distribution in the aquifer in the year of 2022 under Scenario IV conditions.

6.5. Scenario Five

If no discharge occurs from the aquifer or recharge increases by the amount of present discharge in the next 20 years, groundwater values would increase about 0.84 m on the average between 6000 m and 8000 m from the shoreline. Chloride concentration distribution obtained from Scenario V is

similar to present condition. Chloride concentrations show only about 5% increase at distance of 6000 m from shoreline. Change of Cl concentration at a depth of 50 m and 100 m at the distance of 6000 m from shoreline for each scenario is shown in Figure 6.5.

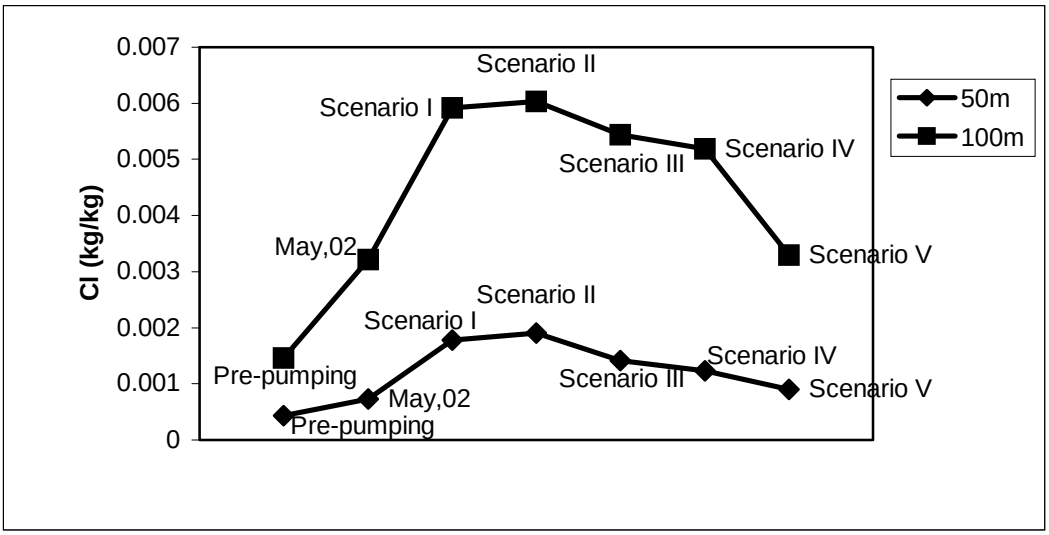

Figure 6.5 Chloride concentration distribution at depths of 50 m and 100 m at a distance of 6000 m from the shoreline at the end of Scenario I, II, III, IV, and V.

CHAPTER 7

CONCLUSION AND RECOMENDATION

Numerical groundwater flow and solute transport modeling have been conducted in order to assess whether seawater intrusion has occurred in the Selçuk sub-basin under present discharge conditions. The results of the simulations reveal that the Selçuk sub-basin undergoes a seawater intrusion. Chloride concentration increased from pre-pumping period of 0.00043 kg/kg to present of 0.00073 kg/kg (corresponding to about 70% increase) at a depth of 50 m and increased from pre-pumping period of 0.00146 kg/kg to present of 0.00322 kg/kg (corresponding to about 120% increase) at a depth of 100 m at the distance of 6000 m from shoreline.

Future prediction simulations suggest that the groundwater quality in the aquifer will further be deteriorated if no water management measures are taken in the Selçuk sub-basin.

If present discharge rate continues in the next 20 years, present groundwater levels would decrease about 0.25 m on the average between 6000 m and 8000 m from the shoreline and chloride concentration would increase to about 0.0018 kg/kg at a depth of 50 m and increase to about 0.0060 kg/kg at a depth of 100 m at the distance of 6000 m from shoreline.

The simulations indicate that unless the present discharge is completely stopped, the seawater intrusion in the sub-basin would continue. The

intrusion would cease if the discharge is completely stopped or alternative water supply is provided as recharge to the aquifer.

These results exhibit the importance of the Beydağ Dam Project which essentially would cause increasing recharge from the neighboring Torbalı-Bayındır sub-basin to the Selçuk sub-basin.

REFERENCES

Barone, F. S., Yanful, E. K., Quigley, R. M. and Rowe R.K., 1989. Effect of multiple contaminant migration on diffusion and adsorption of some domestic waste contaminants in a natural clayey soil. Canadian Geotechnical Journal, 26: 189-198.

Bear, J., 1979. Hydraulics of groundwater. McGraw-hill, New York, N.Y., 567 pp.

Bear, J. and Dagan, G., 1964. Some exact solutions of interface problems by means of the hydrograph method. J. Geophys. Res., 69 (8): 1563–1572.

Bear, J. and Tod, D.K., 1960. The transition zone between fresh and salt waters in coastal aquifers. Hydraul. Lab., Univ. Of California, Berkerley, Calif., Water resource Center Contrib., No. 29, 156 pp.

Bruggeman, G.A. and Custodio, E. 1987. Groundwater problems in coastal areas, Unesco, Belgium, 596 pp.

Cooper H. H., 1959. A hypothesis concerning the dynamic balance of fresh water and salt water in coastal aquifer. J. Geophys. Res. No. 11, 26 pp.

Domenico, P.A. and Schwartz, F.W. 1999. Physical and chemical hydrogeology. John Wiley & Sons, 823 pp.

D.S.İ. , 1973. Küçük Menderes Ovası hidrojeolojik etüd raporu, D.S.İ. Genel Müdürlüğü, Jeoteknik Hizmetler ve Yeraltısuları Daire Başkanlığı, Ankara, 65 pp.

Edelman, J.H., 1972. Groundwater hydraulics of extensive aquifers International Institute for Land Reclamation and Drainage Bulletin V. 13, Wageningen, The Netherlands, 216pp.

Erinç, S., 1978. Changes in the physical environment in Turkey since the end of the last glacial. In The environmental history of the Near and Middle East since the last ice age. Ed: William C. Brice, Chp. 7: 87-110.

Freeze, R. A. and Cherry, J. A., 1979. Groundwater, Prentice Hall, 604 pp.

Glover, R.E., 1959. The pattern of fresh-water flow in a coastal aquifer. J. Geophys. Res., 64 (4): 45–459.

Gül, A., 1967. Küçük Menderes Havzası jeofizik rezistivite etüd raporu, D.S.İ. Genel Müdürlüğü, Jeoteknik Hizmetler ve Yeraltısuları Daire Başkanlığı, Ankara.

Gündoğdu, A., 2000. Groundwater recharge estimation for Küçük Menderes River Basin aquifer system. M.Sc. Thesis, January 2000, Middle East Technical University, 181 pp.

Henry, H. R., 1959. Salt intrusion into fresh-water aquifers. J. Geophys. Res., 64 (11): 1911–1919.

Henry, H. R.,1962. Transitory movements of the salt - water front in an extensive artesian aquifer. U.S. Geol. Surv., Prof. Pap, 450-B, pp. B87–B88.

Henry, H. R.,1964. Effects of dispersion on salt encroachment in coastal aquifers. In: Sea Water in coastal aquifers. U. S. Geol. Surv., Water Supply. Pap. 1613-C, 70–84.

Hubbert, M. K., 1940. The theory of ground-water motion. J. geol., 48 (8): 785–944.

Kooi, H. and Groen, J. 2001. Offshore continuation of coastal groundwater systems; predictions using sharp interface approximations and variable density flow modeling. Journal of Hydrology, 246: 19-35.

Mustak, M., 1937. The flow of homogenous Fluids Through porous Media. Mcgrow-Hill, New York, N.Y., 763 pp.

Nippon, 1996. The study on Küçük Menderes River Basin irrigation project in the Republic of Turkey, Final Report: Volume I: Main Report, Volume II: Annexes, Volume III: Drawings, Nippon Koei Con., Ltd.-Nippon Giken Inc.

Reilly, T.E. and Goodman, A.S. 1987. Analysis of saltwater upconing beneath a pumping well. Journal of Hydrology, 89: 169-204.

Rowe, R.K., Caers, C.J. and Barone, F., 1988. Laboratory determination of diffusion and distribution coefficients of contaminants using undisturbed clayey soil. Canadian Geotechnical Journal, 25: 108-118.

Voss, C., 1984. A finite element simulation model for saturated-unsaturated, fluid-density dependent groundwater flow with energy transport or chemically-reactive single-species solute trandport. U.S.G.S. Water-Resources Investigation Report No: 84-4369, 409 pp.

Voss, C. and Andersson, J., 1993. Regional flow in the basaltic shield during Holocene coastal regression. Groundwater V. 31: 989-1006.

Yazıcıgil, H., Karahanoğlu, N., Yılmaz, K., Gündoğdu, A., Şakıyan, J., Yeşilnacar, E. and Tuzcu, B., 2000a. Revize hidrojeolojik etütler kapsamında küçük menderes havzası yeraltısularının incelenmesi ve yönetimi. Cilt-V Hidrojeoloji. Orta Doğu Teknik Üniversitesi.

Yazıcıgil, H., Çamur, M.Z. and Pusatlı T., 2000b. Revize hidrojeolojik etütler kapsamında küçük menderes havzası yeraltısularının incelenmesi ve yönetimi. Cilt-VI Su kimyası ve kirlilik. Orta Doğu Teknik Üniversitesi.

Yazıcıgil, H., Toprak, V., Rojay, B., Süzen, L. and Yılmaz, K., 2000c. Revize hidrojeolojik etütler kapsamında küçük menderes havzası yeraltısularının incelenmesi ve yönetimi. Cilt-III Jeoloji. Orta Doğu Teknik Üniversitesi.

APPENDIX A

MONITORING WELL STATIC LEVEL DATA

Table A.1. Static level data of well no: 18495. (State Hydraulic works of Turkey)

DATE	STATIC LEVEL	DATE	STATIC LEVEL	DATE	STATIC LEVEL
Aug-73	1.11	Aug-76	0.52	May-86	2.24
Mar-74	1.49	Sep-76	0.52	Oct-86	1.62
Apr-74	2.09	Oct-76	1.12	May-87	2.42
Jul-74	2.01	Nov-76	1.42	Oct-87	-1.93
Aug-74	0.49	Jan-77	2.02	May-88	1.27
Sep-74	-1.01	Feb-77	1.62	Oct-88	0.22
Oct-74	0.59	Apr-77	2.04	May-89	1.32
Dec-74	1.67	May-77	1.82	Oct-89	-0.98
Jan-75	2.59	Jul-77	1.47	May-90	1.74
Feb-75	2.71	Dec-77	1.57	Oct-90	-1.96
Mar-75	2.59	May-82	3.02	May-91	1.19
Apr-75	2.39	Oct-82	2.07	Oct-91	0.34
May-75	2.09	Nov-82	2.12	May-92	-2.16
Jun-75	2.15	Dec-82	2.27	Oct-92	-2.96
Jul-75	1.94	Jan-83	2.17	May-93	2.69
Nov-75	1.77	Mar-83	2.47	Oct-93	-2.06
Feb-76	2.02	May-83	2.47	May-94	0.94
Mar-76	1.62	Oct-83	1.5	Oct-94	-2.06
Apr-76	1.59	May-84	3.72	May-95	2.49
May-76	2.12	Oct-84	1.74	Oct-95	0.74
Jun-76	2.18	May-85	2.17	May-96	3.34
Jul-76	1.77	Oct-85	0.97	Oct-96	1.34

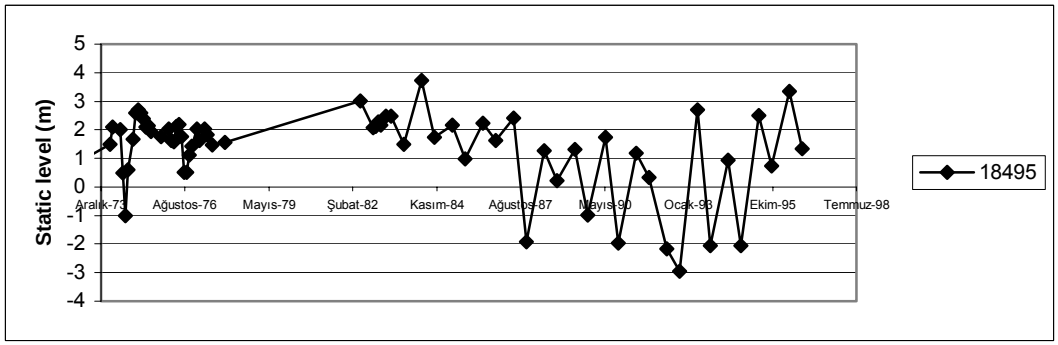

Figure A.1. Hydrograph of well no: 18495.

Table A.2. Static level data of well no: 21381. (State Hydraulic works of Turkey)

DATE	STATIC LEVEL
Oct-76	1.07
May-77	1.95
Jul-77	1.56
Dec-77	2.69
May-82	2.57
Jun-82	2.47
Jul-82	2.19
Sep-82	1.86
Nov-82	2.41
Dec-82	2
Jan-83	2.02
Mar-83	2.37
Aug-83	0.57
Sep-83	0.77

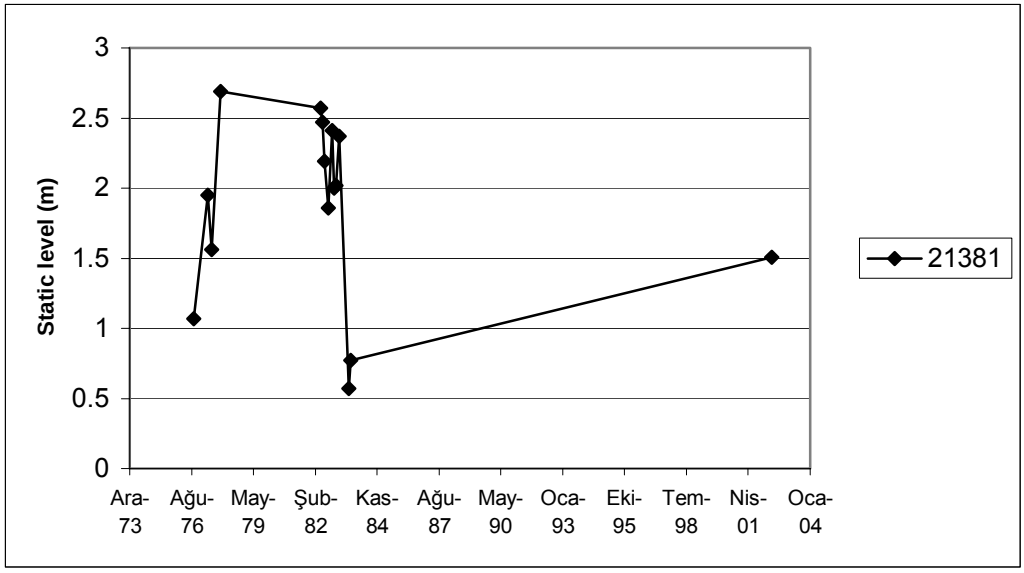

Figure A.2. Hydrograph of well no: 21381.

APPENDIX B

MONITORING WELL EC AND Cl CONCENTRATION DATA

Table B.1. EC (μ/cm) and Cl (mg/l) data of State Hydraulic Works of Turkey.

WELL No	Date	EC	Cl
20047	Feb-76	2064	443.16
20047	Sep-91	1015	143.23
20047	Aug-94	2420	609.08
20047	Sep-95	1296	249.59
20047	Sep-01	1276	248.15
21381	Oct-76	1958	393.53
21381	Sep-91	1277	222.64
21381	Aug-94	1427	283.62
21381	Sep-95	1241	206.34
21381	Sep-01	2690	713.25
22330	Aug-77	2063	443.16
24853	Feb-79	1906	407.71
24853	Sep-91	2200	508.04
24853	Aug-94	2250	524.7
24853	Jun-95	2530	604.12
24853	Sep-95	2540	589.23
24853	Jun-96	1217	116.99
24853	Sep-96	1185	179.04
24853	Jun-97	986	165.92
24853	Sep-97	1281	121.25
24853	Sep-01	2620	725.66
24854	Mar-79	1174	81.54
24854	Sep-91	1133	89.34
24854	Jul-94	1097	104.94
24854	Sep-95	1183	100.69
24854	Sep-01	1165	173
24855	Apr-79	1756	340.35
24855	Sep-91	1237	178.33
24855	Aug-94	870	80.12
24855	Sep-95	894	80.12
24855	Sep-01	1788	446.7
205	Jan-91	729	35.45
221	Mar-91	748.7	40.06
251	Mar-91	770.3	38.99
254	Mar-91	1106.8	80.82
267	Mar-91	758.2	40.77
1029	Aug-88	835.3	45.02
66(K1)	Sep-76	982.3	158.45

Table B.1 (continued)

WELL No	Date	EC	Cl
1000	Jul-60	650	35.81
1895	Aug-73	948	92.18
1895	Sep-91	1092	168.4
1895	Aug-94	1428	273
1895	Sep-95	1493	336.8
1895	Sep-01	981	166.6
20045	Dec-75	757	74.45
20045	Sep-91	821	86.51
20045	Aug-94	1019	147.5
20045	Jun-95	1054	149.6
20045	Sep-95	1028	133
20045	Jun-96	993	133
20045	Sep-96	1237	265.9
20045	Jun-97	938	137.6
20045	Sep-97	972	133
20045	Sep-01	730	88.63
20046	Feb-76	2064	443.2
20046	Sep-91	1752	365.9
20046	Aug-94	2320	590.3
20046	Sep-95	2310	525.1
20046	Sep-01	1206	231.8

Table B.2. EC (μ S/cm) and Cl (mg/l) data of Yazıcıgil et al. (2000b).

Proj No	East	North	Depth	Date	EC	Cl
P1	533500	4203800	90	Jul-98	2830	815.4
P2	531200	4202700	40	Jul-98	2210	545.2
P3	529800	4203500	40-100	Jul-98	1460	
P4	531408	4198641		Oct-98	864	49.4
P5	527436	4201733		Oct-98	3140	732.9
P7	531600	4203900	60	Jul-98	1910	
P8	525100	4204800	38	Jul-98	1390	
P10	528900	4204800	60	Oct-98	4020	
P11	530650	4200415		Oct-98	2280	
P12	527242	4200586		Oct-98	4940	
P13	532696	4201822	80	Apr-99	1801	310.1
P14	528683	4202589		Apr-99	2500	338.8
P15	525257	4204572	Artesian	Apr-99	1460	208.3
P17	529484	4204242		Apr-99	1830	304.5
P18	532319	4201551		Apr-99	2100	215.6
P19	532087	4199485		Apr-99	1000	116.9
P20	527277	4200776		Apr-99	4150	535.2
KS	524161	4204619	spring	Jul-98	6180	1304.6
KS	524161	4204619	spring	Apr-99	6970	695.1
20046	533301	4201252	105	Oct-98	1700	270.2
21381	531017	4200106	70	Oct-98	2320	416.9